2016

Changes in Cytoskeleton Proteins in HSV-1 Infection of J774a.1 Macrophage Phenotype

Riham Abbas Subahi
Wright State University

CHANGES IN CYTOSKELETON PROTEINS IN HSV-1 INFECTION OF J774A.1 MACROPHAGE PHENOTYPES

A thesis submitted in partial fulfillment

of the requirements for the degree of

Master of Science.

By

RIHAM ABBAS, SUBAHI

B.S., Umm Al-Qura University, 2009

2016

Wright State University

WRIGHT STATE UNIVERSITY

GRADUATE SCHOOL

March 24, 2016

I HEREBY RECOMMEND THAT THE THESIS PREPARED UNDER MY SUPERVISION BY Riham Abbas Subahi ENTITLED Changes in Cytoskeleton Proteins in HSV-1 Infection of J774A.1 Macrophage phenotype BE ACCEPTED IN PARTIAL FULFILLMENT OF THE REQUIREMENTS FOR THE DEGREE OF Master of Science.

Committee on Final Examination

Nancy J. Bigley, Ph.D.
Professor of Microbiology and Immunology

Nancy J. Bigley, Ph.D.
Thesis Director

Barbara E. Hull, Ph.D.
Professor of Biological Sciences

Barbara E. Hull, Ph.D.
Director of Microbiology and Immunology Program,
College of Science and Mathematics

Dawn P. Wooley, Ph.D.
Associate Professor, Neuroscience Cell Biology & Physiology Associate Professor, Emergency Medicine

Robert E.W. Fyffe, Ph.D.
Vice President for Research and Dean of the Graduate School

ABSTRACT

Subahi, Riham Abbas. M.S. Microbiology and Immunology Graduate Program, Wright State University, 2016. Changes in Cytoskeleton Proteins in HSV-1 Infection of J774A.1 Macrophage phenotype

The cell cytoskeleton, a unique intracellular matrix found in all eukaryotes, is composed of three main protein structures, microtubules, microfilaments and intermediate filaments. The cytoskeleton maintains cell shape and internal structures providing mechanical support that facilitates intracellular transport (Parker *et al*., 2014). Many viruses such as the herpesviruses use the cytoskeleton system of the cell for infectivity (Henry Sum, M. S. 2015). HSV-1 utilizes the cell cytoskeleton in many steps of its life cycle from entry through assembly to egress (Lyman *et al.*, 2008). During infection, HSV-1 viral proteins cause drastic changes and rearrangement of the cellular actin and cell signaling during viral replication. The goal of this study was to determine the effects of HSV-1 challenge on cell viability, morphology, and levels of tubulin and F-actin in unpolarized and cytokine-polarized murine J774A.1 macrophages at 24, 48 and 72 hours. M1 macrophage phenotype was generated by treatment with interferon-gamma (IFN-γ) and bacterial lipopolysaccharide (LPS); three M2 phenotypes were produced by polarization with interleukin-4 (IL-4) or IL-10 or IL-13. The most prominent change in cell morphology caused by HSV-1 is the formation of small rounded cell shape from the transformed cells (Taylor *et al*., 2011) which was confirmed in this study. Immunofluorescence images of all macrophage subgroups (unpolarized M0, M1, the three M2 phenotypes) after HSV-1 infection were indistinguishable all showing smaller rounded cell shapes. Uninfected M1 cells were flattened, irregularly shaped cells containing visible intracellular vacuoles compared to the rounded cell shape in uninfected M0 or M2 polarized macrophages. Furthermore, uninfected M2 macrophages stimulated by IL-4

showed a combination of morphologies ranging from elongated to rounded cells. Uninfected M2 macrophages polarized by IL-10 or IL-13 displayed a rounded cell type which closely resembled unpolarized (M0) cells. In viability experiments, HSV-1-infected unpolarized cells and polarized M1 inflammatory macrophages exhibited rapid decline in cell numbers compared to unpolarized M0 and M2 anti-inflammatory macrophages polarized by IL-4, IL-10 and IL-13. This reduction in cell viability was expected due to the crucial role macrophages play in viral clearance by producing molecules toxic to both the infecting agent and the cell itself. The relative amounts of tubulin and F-actin microfilaments were evaluated by quantifying the fluorescent intensity of immunofluorescent microscopy images through ImageJ analysis. The majority of uninfected M1 and M2 macrophages subgroups displayed increased levels of tubulin and F-actin compared to the levels seen in uninfected M0 control cells. In contrast, infection by HSV-1 markedly reduced amounts of the immunofluorescent intensity of either tubulin or F-actin 48 hours after polarization and infection of M1 and M2. By 72 hours, the greater amounts of tubulin and F-actin were present in all polarized and infected cells (M0, M1, and the three M2 phenotypes) which may reflect an anti-apoptotic effect of HSV-1 on these cells as described by others (Roizman and Taddeo, 2007) and (Aubert *et al.,*2008).

The specific goals of this project

- This project involved the study of morphology, viability, and cytoskeletal structures in unpolarized and polarized murine J774A.1 macrophages using an antibody α/β- tubulin and a fluorescent stain to detect microfilament (F-actin) phalliodin binding.

- The overall goal of this study was to characterize the microtubules and microfilament (F-actin) structures of the macrophages at three different states: 1) unpolarized M0 state as a control; 2) inflammatory polarized M1 state after treatment with IFN-γ and LPS; and 3) anti-inflammatory polarized M2 state after treatment with either IL-4 or IL-10 or IL-13 and with or without HSV-1 infection.

- Control (unpolarized) and polarized cells were examined microscopically at 24, 48, and 72hrs following the treatment using fluorescently-labeled antibodies to detect tubulin and F-actin in the cells.

HYPOTHESIS

J774A.1 murine macrophages cells in the naïve state (M0), and polarized M1 and M2 phenotypes will display changes in cell morphology, decrease in polarized M1 state viability and a reduction in immunofluorescent intensity staining of microtubules (tubulin) and microfilaments (F-Actin) at 24, 48, 72 hours following HSV-1 infection. These characteristics will distinguish between the M1 and M2 phenotypes.

TABLE OF CONTENTS

LIST OF FIGURES

LIST OF TABLES

LIST OF ABBREVIATIONS

BSA	Bovine serum albumin
DMEM	Dulbecco's modified eagle's medium
F-actin	Filamentous actin
gD	Glycoprotein D
HSV	Herpes simplex virus
IFs	Intermediate filaments
IFN-γ	Interferon-gamma
IL	Interleukin
iNOS	Inducible nitric oxide synthase
LPS	Lipopolysaccharide
MHC	Major histocompatibility complex
MOI	Multiplicity of infection
PBS	Phosphate buffered saline
qROI	Qualified region of interest
SOCS	Suppressor of cytokine signaling
TNF-α	Tumor necrosis factor-alpha

DEDICATION

I would like to dedicate this thesis project to

- My parents:

Thank you my Mom and Dad for all of your undying love, support, and inspiration. Thank you for giving me strength and providing me with a constant encouragement throughout my years of studies.

- My husband:

Thank you for believing in me, for allowing me to further my studies , and leaving your job back in our country and coming with me to peruse my dream. Please do not ever doubt my dedication and my endless love for you

- My children:

Thank you Lurin, Yousuf and Yaseen for being around me and being patient with me during my busy times in the school far away from you by my body but not my soul. You are my inspiration, I owe everything to you. Hoping that with this research I have proven to you that there is nothing impossible and you will be able to chase your dreams and be the best version of yourself my sweethearts.

ACKNOWLEDGEMENT

I would like to sincerely thank my advisor, Dr. Nancy J. Bigley for her guidance and support throughout this journey, and especially for her time she spent for helping me to achieve my research goals and to finish this study. I would also like to thanks my program director, Dr. Barbara E. Hull for her guidance and support that I believed I learned from the best. I must also thank Dr. Dawn P. Wooley for serving as a member on my thesis committee and for her advices and suggestions.

To all my family and my friends, thank you for your help and encouragement me in my many disappointed moments. Furthermore, I would like extend a special thank you to my lab mate Caitlin for editing my thesis and providing crucial feedback.

Thank you, Allah, for always being there for me and let me finish this study successfully.

INTRODUCTION

Herpes simplex virus type 1 and cytoskeleton

Herpes simplex virus type 1 (HSV-1) is widespread in the human population and affects about 80% of the adult population worldwide (Casrouge *et al.,* 2006; Huang *et al.,* 2010). HSV-1 has a linear double-stranded DNA genome around 100 kbp (Zaichick *et al.,* 2011). The signs and symptoms of HSV-1 infection are lesions, cold sores, keratitis and, rarely, encephalitis. (Johnson et al., 2012; Frampton et al., 2005; Zaichick *et al.,* 2011). The HSV-1-infected individual can develop a latent infection in the neurons of the peripheral ganglia (Wakimoto *et al.,* 2003). HSV-1 has an amorphous layer of proteins known as tegument and a lipid envelope that contains at least 11 glycoproteins which are involved in a variety of roles of the virus life's cycle, like attachment and entry (Zaichick *et al.,* 2011). HSV-1 can persist in many cell types such as epithelial cells, especially the keratinocyte, which is the first cell type to be infected in a human (Frampton *et al.,* 2005). Depending on the cell's receptors, HSV-1 can enter the cells either by endocytosis or by fusing within the plasma membrane (Ghadah and Deepak, 2011). HSV-1 glycoprotein D (gD) is necessary in host-receptor interaction for virus entry into cells and is responsible for fusion with cell membrane (Frampton *et al.,* 2005). Following binding, HSV-1 restructures the host cytoskeleton using different cellular signals to enlist the cytoskeleton for virus replication and intracellular trafficking (Turowska *et al.,* 2010; Campbell *et al.,* 2005).

HSV-1 utilizes the cell cytoskeleton in many steps of its life cycle from entry through assembly to egress (Lyman *et al.,* 2008). Microtubules are polymers of α- and β-tubulin which form the spindle fibers for separating chromosomes during mitosis (Parker *et al.,* 2014). Microtubules also play a significant role in the cell proliferation at many stages of the viral life cycle. HSV-1 capsids travel long distance from the site of entry to the nucleus through microtubules transport machinery (Lyman *et*

al., 2008). Microtubules have two polymeric ends that govern directional transport along microtubules. The plus end guides the capsids toward plasma membrane (anterograde transport), whereas the minus end that directs capsids toward the nucleus (retrograde transport) (Lyman *et al.,* 2008) (Figure 2). During HSV-1 infection, the capsid travel direction throughout microtubules is directed by two classes of molecular motors either dynein or kinesin depending on the polarity. Microfilaments, the thinnest filaments of the cytoskeleton, are composed of polymerized filaments (F-actin). Each monomer subunits (G-actin) bound to ATP molecules and intertwined to form stabilized polymeric filamentous actin (F-actin) (Spear, M., & Wu, Y. 2014; Taylor at el., 2011). During internalization, herpesviruses depend on actin structures in both entry into the cell and exit (Clement et. al., 2006; Turowska *et al.,* 2010). Like microtubules, F-actin has an intrinsically polar made of plus (barbed) ends and minus (pointed) ends (Lyman *et al.,* 2008). One study showed that the cell microfilaments intensity levels start to decrease at 4 hours after HSV-1 infection of Vero cell with a continuous decrease over the next 12 to 16 hours (Lyman *et al.,* 2008). Viral proteins during infection cause drastic changes and rearrangement of the cellular actin and cell signaling during the cell proliferation. The most prominent changes in cell morphology caused by many viruses is rounded cell shape (Taylor *at el.,* 2011). The initial binding of HSV-1 gD to the cell surface receptor within nectin-1 influence Rho GTPase family cell's signaling to rearrange the morphology of actin filaments. The interaction between HSV-1 and actin involves Rho GTPases signaling system during different phases during HSV-1 cycle of replication: entry, replication and assembly, and maturation and egress (Favoreel *et al.,* 2007) (See figure 1).

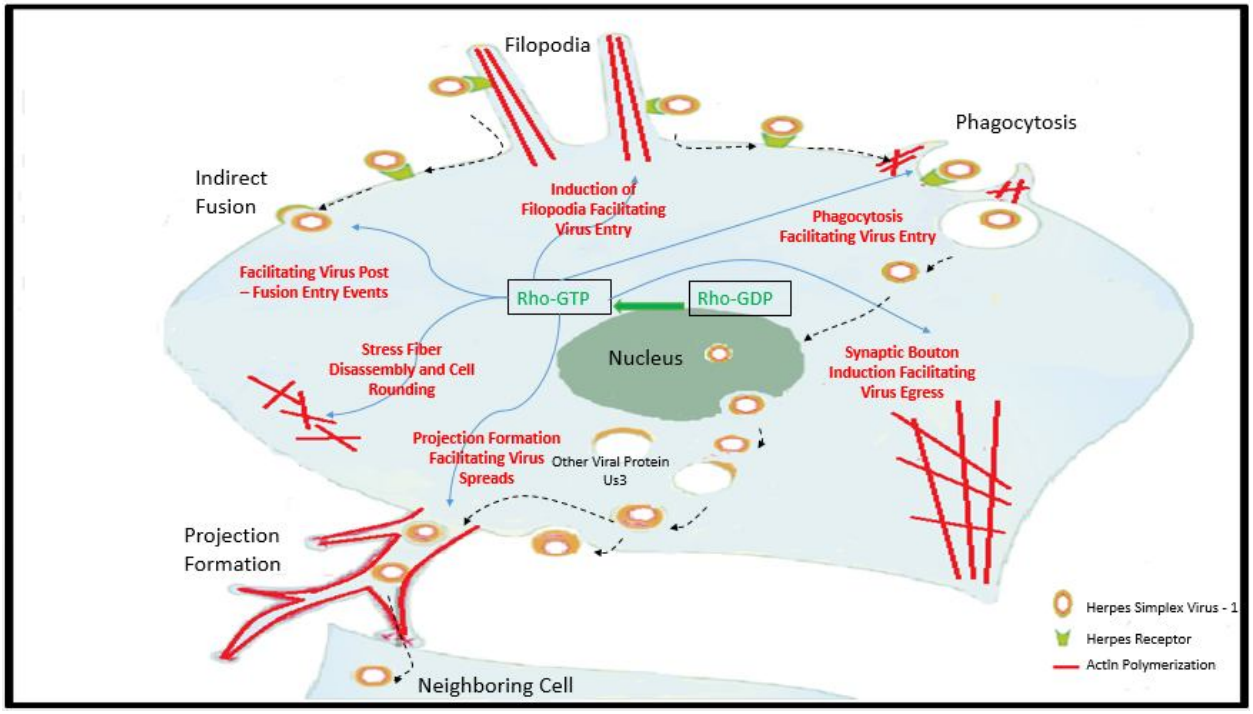

Figure 1: The infection cycle of herpesvirus with involvement of actin and Rho GTPase signaling pathways

Shows herpes virion entry to the plasma membrane by either fusion or endocytosis depending on actin polymerization. Following the virus attachment, Rho GTPase signaling pathways have been activated and lead to many downstream effects like formation of filopodia; Moreover, shows the incorporation of actin polymerization even through the final stages of herpesvirus replication like budding and disassembly via US3-mediated which result of de-polymerization of actin stress fibers. US3-mediated can generate projection formation and enhance the intercellular spread of herpesvirus. **(Redrawn from Favoreel *et al.*, 2007)**

HSV-1 and Macrophages

Macrophages which develop from monocytes are the central regulator of the immune response in both innate and adaptive immunity (Mosser and Edwards, 2010). Macrophages are phagocytic cells that are capable of engulfing and digesting foreign substances, and help in repairing damaged tissue (Martinez and Gordon, 2014; Wang *et al.*, 2014). Macrophages can direct the host immune system to produce specific pro and anti-inflammatory cytokines that cause alterations in cellular homeostasis and inhibit virus replication. The binding macrophage to HSV-1 toll-like receptor (TLR) initiates the MyD88 signaling pathway that causes the production of an anti-viral interferon (Wang *et al.*, 2011).

Furthermore, macrophages can express a variety of surface receptors recognizing signals and recruiting vital components of the host immune system (Martinez, 2008). In the event of HSV-1 infection, the first host response to HSV-1 is mediated by macrophages and natural killer cells. Macrophages can eliminate HSV-1 infection by different mechanisms which include the production of reactive oxygen species (ROS) and nitric oxide (NO), (Gabhann *et al.,* 2014). There are two different states of polarized activation for macrophages to fulfil their functions: classically activated macrophages (M1) and alternatively activated macrophages (M2). Naïve macrophages are polarized to M1 state in the case of inflammatory stimuli and danger signals to be able to fight pathogens. On the other side, M0 macrophages are polarized toward an M2 phenotype to promote wound healing (Mcwhorter *et al.,* 2013).

In this study the J774A.1 murine macrophage cell line was the selected candidate for studying the pivotal role of macrophages during HSV-1 infections. The hypothesis of this study was to determine the effects of HSV-1 challenge on cell viability, morphology, and the levels of tubulin and F-actin in M1 and M2 macrophages at 24, 48,and 72 hours. J774A.1 murine macrophages cells in the naïve state (M0), and polarized M1 and M2 phenotypes will display distinguishable characters following HSV-1 infection.

REVIEW OF LITERATURE

HSV-1

Herpes simplex viruses (HSV) are members of the alphaherpesvirus subfamily of herpesviruses (Geraghty *et al.,* 1998). They are large viruses which consist of two types: Herpes simplex virus type-1 (HSV-1) and Herpes simplex virus type-2 (HSV-2). These viruses are known to be neurotropic and cause neurological diseases by infecting the nervous system of the victim (Ghadah and Deepak. 2011). HSV-1 is a linear double stranded DNA virus that affects about 80% of the young adult population worldwide (Casrouge *et al.,* 2006; Huang *et al.,* 2010). During primary and recurrent infections, an infected person can develop cold sores and lesions in the peripheral and central nervous systems (Huang *et al.,* 2010). HSV-1 can also infect the cornea leading to corneal blindness and in much more complicated cases can lead to fatal encephalitis (Johnson *et al.,* 2012). During initial infection, HSV-1 can replicate in epithelial cells of peripheral tissues, such as the cornea and the skin. In addition, it can replicate in either peripheral sensory ganglia or the central nervous system where the virus may establish lifelong latent infections in the hosts. HSV can establish latency infection in the host sensory neurons without displaying any symptoms in the infected individual (Wakimoto *et al.,* 2003). Exposure to ultraviolet (UV) irradiation, emotional stress, fever, or immunosuppression can activate the latent virus and cause recurrent infection. The virus can replicate and initiate a lytic cycle in epithelial cell by being transported through neuronal axons (Bigley, 2014). Many studies demonstrate that HSV has the ability to enter into host cells by two major entry routes. The first one is called endocytosis where the virus triggers fusion with the phagocytic membrane. The other one is a pH independent or direct fusion at the plasma membrane of the host cell (Rahn *et al.,* 2011; Ghadah and Deepak. 2011). HSV has a number of viral glycoproteins surrounding the tegument that help in

attaching the virus to the cell surface of the host; these proteins molecule gB, gC, gD, gH, gK, gL, and gM. The virus attaches to cell membrane receptors by interaction of the viral glycoproteins gB and gC with heparan sulfate proteoglycans (HSPG) on the surface of the host cell (Rahn *et al.,* 2011). Virus fusion with the plasma membrane of the host cell receptor is facilitated by five viral glycoproteins: gB, gC, gD, gH and gL (Geraghty *et al.,* 1998). The Glycoprotein D (gD) is necessary in host-receptor interaction for virus entry by endocytosis route.

The role of IFN-γ as antiviral in fighting HSV-1

Because HSV-1 depends on the cytoskeletal protein transport system, IFN-γ, an anti-viral agent, tends to suppress actin remodeling in the host cell (Bigley, 2014). IFN-γ stimulates the cytoskeletal network for transporting MHC molecules in antigen-presenting cells leading to an increase in expression of both class I and class II MHC molecules on the cell surface (Barois *et al.,* 1998). A profound effect of IFN-γ on the cell cytoskeleton is to induce a higher basal level of F-actin and activation of Rac-1 (GTPase), which may cause a decrease in phagocytosis by macrophages (Frausto-Del-Rio *et al.,* 2012). Another indirect effect of IFN-γ on the cell cytoskeleton is to inhibit monocyte migration by suppressing actin remodeling of the cytoskeleton and polarization in response to chemokine CCL2, a STA1-dependent process modulating activity of Pyk2, JNK, and the GTPases Rac and Cdc42 (Hu, Y., *et al.,* 2008). Moreover, the upregulation of SOCS1 and SOCS3 expression by IFN-γ promote the stability of microtubule network (Bigley, 2014) (Figure 2).

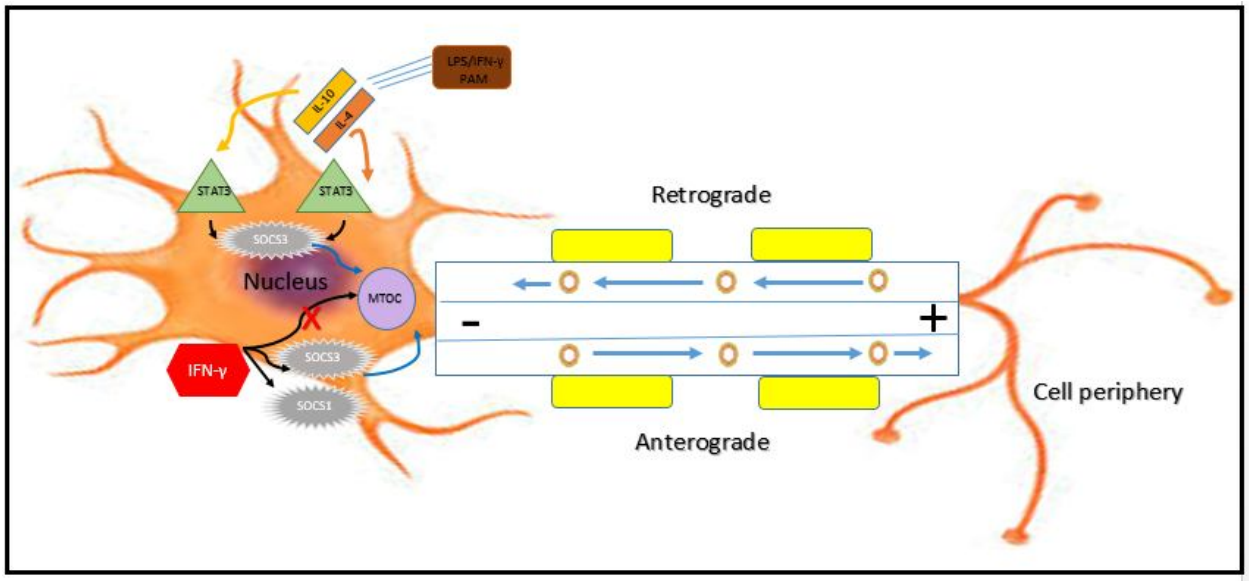

Figure 2: Microtubule trafficking system and the effect of IFN-γ on neuron cell microtubules.

Anterograde transport by microtubules moves the HSV-1 capsids toward plasma membrane, whereas retrograde transport by microtubules directs HSV-1 capsids toward the cell nucleus. IFN-γ results of microtubules stabilization by upregulating the expression of SOCS1 and SOCS3. **(Redrawn from Bigley, 2014)**

Cytoskeleton

Cell cytoskeleton is an intracellular matrix found in all eukaryotes which supports cell morphology and function. It is composed of three main proteins - microtubules, microfilaments and intermediate filaments (Parker *et al.,* 2014). Viruses such as herpesviruses and Japanese encephalitis virus use the cytoskeleton system of the cell for infectivity (Henry Sum, M. S. 2015). Microtubules and microfilaments play a diverse role in the cellular processes like cell division, adherence, migration, and cell transport (Roberts *et al.,* 2011).

Microtubules, microfilaments, and intermediate filaments

Microtubules are polymeric proteins form hollow cylindrical structures and are composed of α- and β-tubulin. Microtubules play a significant role in cell proliferation at many stages of the viral life cycle.

Microtubules form the mitotic spindle which physically pulls the chromosomes inside the nucleus and allows separation of the original cell into two identical daughter cells (Parker *et al.,* 2014). Microtubules distribution inside cells depend on many factors such as ATP levels, posttranslational modification of tubulin subunits, and microtubule-associated proteins. Microtubules also play a role in the movement of HSV-1 capsids from the cell periphery to the nucleus termed as long destination. During HSV-1 infection, the capsid travel direction throughout microtubules is governed by two classes of motors dynein and kinesin (Sodeik *et al.,* 1997). Microtubules have two ends one called the plus end which moves the capsids toward plasma membrane (anterograde transport), whereas the other end is known as the minus end that directs capsids toward the nucleus (retrograde transport). The plus end is dynamically instable because it can grow and shrink rapidly, while minus end relatively stable. VP22 tegument is one of the protein that HSV-1 virion use to facilitate interaction with microtubule cytoskeleton (Campbell *et al.,* 2005). One study noticed some changes in cytoskeletal dynamics when mouse neuronal cell cultures were infected with HSV-1 (Zambrano *et al.,* 2008). Microtubules have an important role in the functional processes of neurons such as neuronal cytoskeletal modifications, neurite disruption and neurodegeneration when the neuron cells were infected with HSV-1 in vivo (Zambrano *et al.,* 2008).

Microfilaments are dynamic proteins composed of polymerized filaments F-actin (Spear, M., & Wu, Y. 2014). Each monomer subunits (G-actin) bound to ATP molecules and intertwined to form stabilized polymeric filamentous known as F-actin. F-actin can form more complex structures such as actin arrays or networks when it joins other actin filaments. During infection, HSV-1 utilizes host actin and actin-associated myosin motors during entry into cells. HSV-1 relies on the host machinery to replicate and disseminate (Roberts *et al.,* 2011). Rho GTPase signaling which is activated by nucleotide exchange of inactive GDP to active GTP is required to regulate F- actin within the host cell

during viral infection. RhoA, Rac1 and Cdc42 are the three common Rho GTPases forms involved in herpesvirus infections. RhoA is associated with the generation of actin stress fibers, Rac1 with lamellipodia and ruffling, and Cdc42 with filopodia; these factors are critical for mediating cytoskeletal changes during viral infection (Spear, M., & Wu, Y. 2014; Roberts *et al.,* 2011).During internalization, many viruses depend on actin structures in some way. For example, HSV-1 needs RhoA, tyrosine kinase, and actin-dependent phagocytosis for viral entry (Clement C *et al.,* 2006). Similarly, macrophages require RhoA signaling by actin, Rac1 and Cdc42 for phagocytosis entry mode (Roberts *et al.,* 2011).

Intermediate filaments (IFs) are a staggered tetrameric polypeptides composed of smaller monomer subunits where all twist together and form more stable (strongly bound) rope-like structure (Lyman *et al.,* 2008). IFs have an intermediate size comparing to actin filaments and microtubules with an average diameter of 10 nanometers (Lyman *et al.,* 2008). All body cells have an IFs on the cytoskeleton, but they differ on the types of protein subunits for example: neurofilaments (neurons cell), desmin filaments (muscle cells), Keratin (epithelial cells), vimentin (multi cell types) and frequently co-localize with microtubules, and lamins (all cell types) and support the nuclear membrane envelope structural (Lyman *et al.,* 2008). IFs responsible in the maintenance of cell-shape and provide tensile strength for the cell. Opposing to actin and microtubules, IFs do not serve as transporter machinery for intracellular components (Lyman *et al.,* 2008).

Macrophages

The origin of macrophages, distributions, and functions

Macrophages are white blood cells derived from blood monocytes which undergo further differentiation from bone marrow in the peripheral bloodstream. After that, they leave the bloodstream circulation and migrate into the tissues to differentiate into macrophages and dendritic cells (DCs) by granulocyte macrophage colony stimulating factor (GM-CSF) and macrophage colony stimulating factor (M-CSF) (Stefater *et al.,* 2011). Macrophages are phagocytic cells that capable to engulf and digest foreign substances that enter the blood (Martinez and Gordon, 2014). Beside phagocytosis, macrophages can also play a role in repairing damaged tissue (Wang *et al.,* 2014). Within the host, macrophages can express a variety of surface receptors recognizing signals and recruiting a vital component of the host immune system (Martinez, 2008). Macrophages can also play critical functions in both innate and adaptive immunity (Mosser and Edwards, 2010). Macrophages are found in various tissue such as connective tissue (histiocytes), skin (histiocytes, Langerhans cells), liver (Kupffer cells), lungs (alveolar macrophages), bone (osteoclasts), and the central nervous system (microglia) (Wang *et al.,* 2014) .They are able to alter their function and phenotype depending on the receptor interaction and the cytokines present in the surrounding environment. Therefore, macrophages are best defined depending on their location and specific functional activities (Wang *et al.,* 2014).

Macrophage subsets and phenotypes

The ability to differentiate into different macrophage subpopulations is known as macrophage "M1/M2 polarization". There are two different states of polarized activation for macrophages similar

to T cells, there are some activating macrophages called (pro-inflammatory) and some suppressive macrophages termed as (anti-inflammatory)(Martinez and Gordon, 2014)(Figure 3).

Classically activated (M1) macrophages encourage inflammation by converting arginine to a toxic nitric oxide, and the alternatively activated (M2) decrease inflammation and encourage tissue repair by metabolizing arginine molecule to ornithine (Gabhann *et al.,* 2014; Davis *et al.,* 2013). (IFN-γ combined with LPS polarize naïve macrophages towards the M1 phenotype macrophages and secrete tumor necrosis factor-α (TNF-α), IL-12, and IL-23. This helps to drive antigen specific TH1 and TH17 cell inflammatory responses to become antimicrobial M1 and become phagocytosis cell that able to clear the invading microorganisms (Gabhann *et al.,* 2014; Davis *et al.,* 2013).

On the other hand, IL-4 or IL-13 polarizes the naïve macrophages towards the M2 phenotype that synthesizes anti-inflammatory cytokines like TGF-b1 and IL-10 that lead to tissue repair and immunosuppression during inflammation (Gabhann *et al.,* 2014). IL-4 inducing the M2 state by activating STAT6 through the IL-4 receptor alpha (IL-4Ra) which lead to activates JAK1 and JAK3. IL-10 promotes M2 phenotype via activating STAT3 through IL-10R receptor (Gabhann *et al.,* 2014). Moreover, based on gene expression profiles, M2 macrophages can be further subdivided: M2a, M2b, and M2c (Martinez and Gordon, 2014). There are different stimuli for each subsets: The M2a subsets stimulated by IL-4 or IL-13. The M2b stimulated by IL-1R receptor ligands or exposure to immune complexes plus Toll-like receptor. The M2c stimulated by IL-10 and glucocorticoid hormones (Martinez and Gordon, 2014). Macrophages in vitro are able to transition from one phenotype to the other continuously in response to cytokines (Davis *et al.,* 2013). This re-polarization from M2 to M1 state usually occurs at the level of gene expression, protein, metabolite, and microbicide activity (Wang *et al.,* 2014). The difference in the two functionally macrophages populations is important

clinically because each macrophage subtypes seems to be motived in certain disease processes such as atherosclerosis disease (Stöger *et al.,* 2012; Davis et. al., 2013; Xu et. al., 2014). As a result the body should have a balance between pro-inflammatory and anti-inflammatory macrophage populations. Stöger *et al.,* 2012 study concluded that an imbalance between M1 and M2 phenotypes lead to a higher risk of cardiovascular diseases.

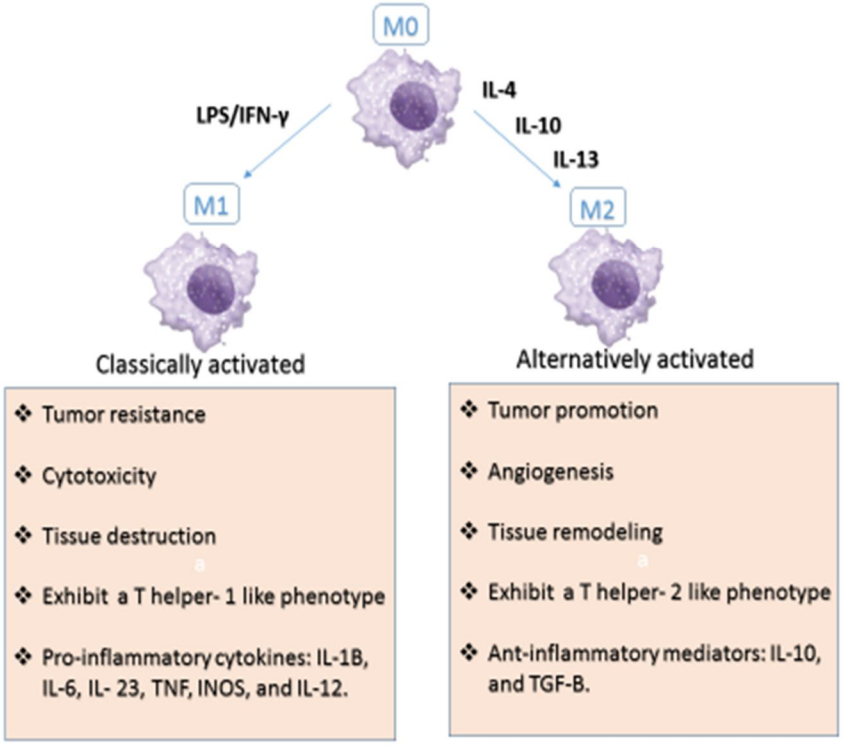

Figure 3: Macrophage polarization and properties functions.

A naïve state (M0) separate to M1 and M2 upon specific stimuli. M1 cells are induced by a combination of LPS and the pro-inflammatory cytokine IFN-γ, whereas M2 cell activated by IL-4, IL-10, or IL-13. **(Redrawn from Quinn et al., 2012*)***

MATERIALS AND METHODS

Cell line maintenance

The murine 774A.1 macrophage cell line, a reticulum cell sarcoma derived from an adult female BALB/cN mouse, was purchased from the American Type Culture Collection (ATCC® TIB-67™, Manassas, VA), and used in this study. The cells are mostly-adherent and maintained in a standard culture medium prepared from Dulbecco's Modified Eagles Medium (DMEM; HyClone, Logan, UT) supplemented with 10% heat inactivated fetal bovine serum (FBS; Fisher Scientific, Pittsburgh PA) and a combination of 1% penicillin/streptomycin antibiotic (MP Biomedical, LLC). Cells were grow in 100 mm x 20 mm cell culture treated Petri dishes (BD Biosciences, San Jose, CA). The cultures were grown in an incubator in an atmosphere of 5% CO2 at a temperature of 37°C. Cells were maintained by sub-culturing two to three times weekly. Cell counts and viability staining were performed using Trypan Blue exclusion test.

Virus

HSV-1 (syn17+) (originally supplied by Dr. Nancy Sawtell, Children's Hospital Medical Center, Cincinnati, OH) was replicated in Vero cells (CCL-81, ATCC). Cells were infected with 0.1 multiplicity of infection (MOI).

Polarization treatment

Macrophages J774A.1 cell were grown to approximately 70% confluency (by observation under the microscope at 40X magnification). Then, the culture medium was replenished with IFN-γ (20 ng/mL) and LPS (100 ng/mL) conditioned media to induce the cells to M1 phenotype.

The M2 phenotype was induced by treatment with 20 ng/ml of either IL-4 or IL-10, or IL-13 (10 ng/ml). These murine cytokines (IFN-γ, IL-4, IL-10 and IL-13) were purchased from Peprotech, Rocky Hill, NJ; LPS was purchased from Chondrex, Redmond, WA. Cultures were allowed to polarize for 24, 48 or 72 hours. Then, cells were collected from the culture dishes using a cell scraper to analyze cell viability, morphological changes, and cell cytoskeleton by immunofluorescence microscope.

Trypan blue exclusion test (Hemocytometer method)

Trypan Blue staining was performed during cell culture to ensure continued viability of cells between passages. Macrophage J774A.1 cells were grown to 70% confluency (by observation under the microscope). Untreated (unpolarized) cells were used as experimental controls. At 24, 48 or 72 hours cells were detached and collected from the 6-well cluster plates and centrifuged at 15,000 revolutions per minute (rpm) at 4˚C for 5 minutes. After centrifugation, cells were suspended in 1 mL of 10% culture DMEM medium. A hemocytometer was cleaned with 70% ethanol and a 20mm glass coverslip was placed over the counting area on the hemocytometer. The cells were stained with trypan blue (Fisher Scientific, Pittsburgh, PA) at a dilution of 1:2 ratio. 10µl of the cell suspension was diluted into trypan blue twice and 10µL of the cell-stain mixture was pipetted into the loading channel on the hemocytometer. Live cells and dead cells were counted separately from the four, sixteen square grids on the hemocytometer. The live cells were identified by excluding the stain and appear white, while dead cells take up the stain and appear blue. The following equation was used to calculate the percent of cell viability:

Percentage of Cell Viability = [Live cells count / Total cells count (Live +Dead)] X 100.

Immunofluorescent staining

The staining procedure in this study was adapted from the study by Xiao and Samulski (2012). Cells were grown on a sterilized 12 well chambers on removable microscope glass slides (Ibidi, Madison, WI) to approximately 50% confluency, at which time either IFN-γ and LPS combined (M1) or IL-4, IL-10, or IL-13 (M2) were added to cell with or without HSV-1 virus for 24, 48 and 72 hours. Untreated (unpolarized) cells were used as an experimental controls. Following the polarization treatment, cells were rinsed with warmed phosphate buffered saline (PBS) (pH: 7.4) for three times, five minutes per wash, to remove non-adherent cells. Then, cells were fixed using 4% paraformaldehyde solution in PBS for 15 minutes at room temperature. Then, fixative was aspirated and cells were rinsed with 1X PBS three times for five minutes per rinse. Cells were then permeabilized using 0.25% Triton X-100 in PBS for 5 -10 minutes at room temperature followed by washing with 1X PBS three times for 5 minutes. After permeabilization, cells were blocked with 5% Goat serum, 3% BSA and 0.05 % Tween solution in PBS for 1-2 hours at room temperature. Following blocking, the primary antibody against tubulin (Cell Signaling Technology, Danvers, MA,) and Texas Red-Phalloidin X (Life Technologies, Carlsbad, CA) to stain F-actin were diluted in PBS and added as specified by the manufacturers (Table-1). The 12-well slide chambers were then incubated overnight at 4˚C. Next day, both α/β- Tubulin Antibody and Texas Red-Phalloidin X were aspirated, and cells were rinsed with PBS three times for 5 minutes per rinse. The secondary antibody (Rabbit IgG Fab'2 Goat anti-Rabbit Polyclonal antibody purchased from LifeSpan BioSciences, Seattle, WA) was added to the same cells with a dilution as recommended by the manufacturer (Table-1) for 1hr in the dark at room temperature. After 1hrs incubation, the secondary antibody was aspirated and each well was washed six times with PBS for 3-5 mins per wash.

Then, cover slips were mounted on chamber slides using Vectashield mounting medium (VECTOR LABORATORIES, Burlingame, CA). The slides were allowed to dry for 20-30 minutes before they were examined under the fluorescence microscope.

Table 1: Summary of the antibodies and staining dilutions:

Antibody/Stain	Dilution
A/B- Tubulin Antibody	1:50
Texas Red-Phalloidin X	1:40
Rabbit IgG Fab'2 Goat anti-Rabbit Polycolonal Antibody	1:500

Image analysis and quantitative procedures

Visualization of the stained chamber slides was performed on an Olympus inverted fluorescence microscope in the imaging facility core located at Wright State University. The optimal wavelengths found for these assays were TRITC (tetramethylrhodamine, red) 500ms and FITC (Fluorescein isothiocyanate, green) 1900ms. The green (FITC) fluorescent intensity represents the level of tubulin staining, while the red (TRITC) fluorescent intensity represents the level of F-actin staining. Optical and software settings were identical when capturing images. The captured immunofluorescent images were analyzed using ImageJ software (National Institutes of Health, http://imagej.nih.gov/ij/) to detect the relative cytoskeletal changes at 24, 48 and 72 hours. This software aided us to isolate the qualified region of interest (qROI) of the fluorescent, exclude uneven background and artifacts, and quantify number of cells. The aim of the image processing steps was to isolate the fluorescence that best represents the presence of either tubulin or F-actin. Processing is based on the concept of lookup tables (LUT). The target metrics are total ROI area (square. pixels) and cell count. These values were found in ImageJ:

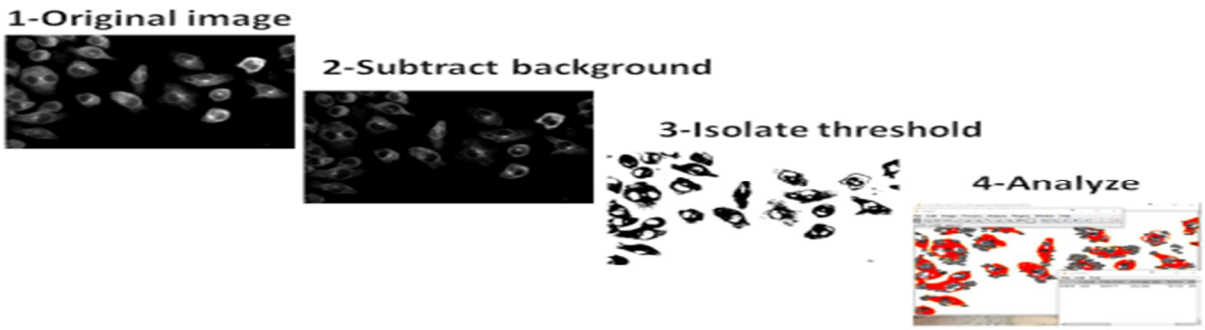

Figure 4: ImageJ processing steps and analysis

The image processing and analysis steps:

First, it was necessary to correct the uneven background after converting the single-color image to eight-bit image. Background subtraction is very important steps when quantifying image intensities; however, subsequent operations on artifacts pixels can be easily done without background interference (Figure 1). Next, before measuring the fluorescence intensity of an image, the pixel values (bins 0-255) of the exclusion regions must be identified. The two exclusion regions are the very black areas like background and the very bright (saturated) artifacts spots. Repeated measurements identified that pixel values from 0-19 represent black and values from 112-255 are present only in the artifacts. In each image, the final range of pixel values representing the ROI were bins 20-111. We limited the total area in the image that contained qualifying pixel intensity after isolating the threshold (ROI). Within the ImageJ threshold feature, the pixel values are fixed to the 20-111 range. At this point, the image is composed of area that will or will not be counted in analysis. After that, image analysis techniques are used to measure the total area restricted within these ROI "islands" and other properties related to the size and distribution. The measure particles function within the ImageJ software calculates the area of individual ROI and provides an image total. Lastly, if the pixel intensity is held constant, an image with more or less cells should have greater or lesser area of ROI. So, normalizing an image's ROI area with the cell count provides a more accurate estimate of tubulin and F-actin intensity per cell. If the normalized (nROI) is reduced from one image to the next, it is reasonable to conclude that only the different experimental conditions contributed to the reduction. To get a reliable quantification, it is necessary that F-actin and tubulin images for each picture were taken from the same spot to compare them.

A)

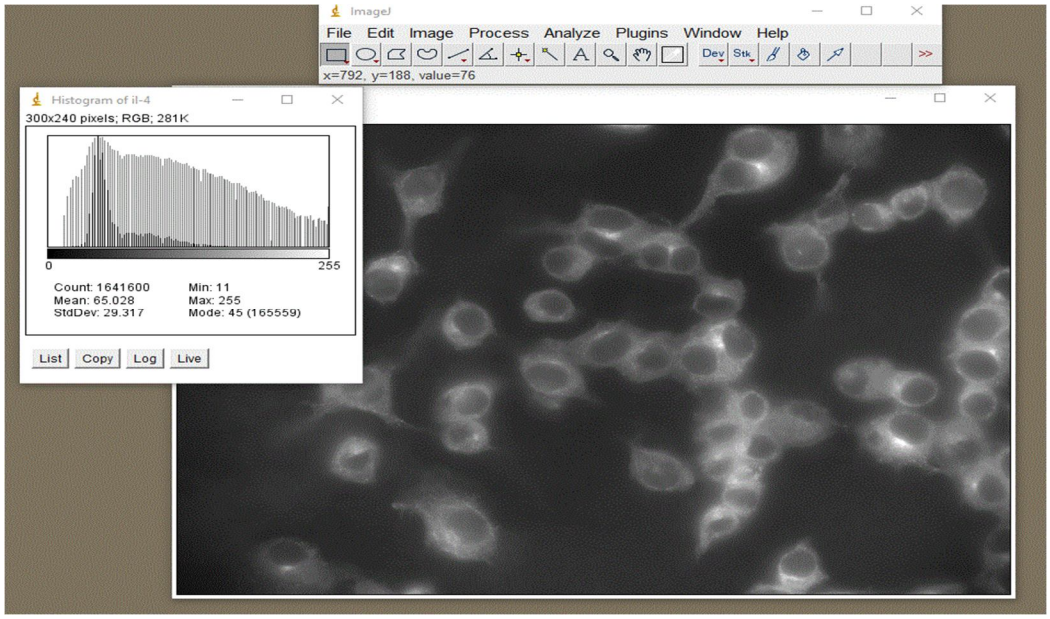

B)

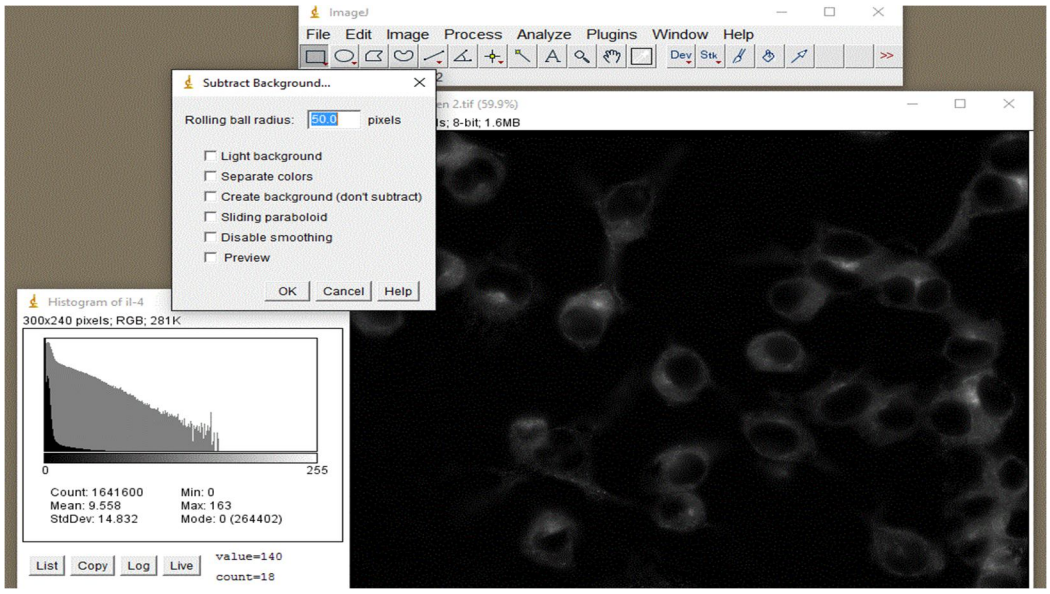

Figure 5: An example of sample background subtraction using an ImageJ software to analyze the intensity of immunofluorescent staining in macrophage J774A.1 cells

A) Original image and histogram of macrophage cells treated with IL-4 and HSV-1 virus and stained with α/β-tubulin antibody to show tubulin intensity. B) Image shown in (A) with background subtracted and associated changes to the histogram.

Statistical analysis

For each different treatment and time point at least a triplicate sample were used to measure cell viability, and tubulin or F-actin immunofluorescent staining intensities. Sigma Plot 12.0 software was used to create graphs and perform statistical analysis. The statistical significance of differences between testing and control experimental groups was analyzed by one way ANOVA and T-test. P-values equal to or less than 0.01 were considered to be statistically significant, and data are represented as the mean ± standard error of the mean. ImageJ was used to process images for statistical analysis as described above.

RESULTS

The cell viability of unpolarized and polarized murine macrophages after 18, 24, and 48 hours prior to and after HSV-1 infection

Cells viabilities prior to HSV-1 Infection

J774A.1 macrophages were treated with IFN-γ (20 ng/mL) and LPS (100 ng/mL) to polarize the cells to the M1 state, or with similar concentrations of IL-4, IL-10, or IL-13 (20 ng/mL) to polarize cells to M2 state. At the initiation of polarization, cells were infected with HSV-1 (MOI 0.1) to see the virus effects on cell viability. Both uninfected and HSV1-infected polarized and unpolarized cells were examined for viability at 24, 48, and 72 hours following polarization. To determine the number of live versus dead cells the viability of macrophages were evaluated by the trypan blue staining assay as described Materials and Methods section.

M1 polarized macrophages showed a significant decrease in viability compared to unpolarized M0 cells (Figure 6A, 7A, 8A). Compared to M0 cells at 24, 48, and 72 hours, viabilities of polarized M1 macrophages were 20% less ($p < 0.001$), 30% less ($p < 0.001$), and 85% less ($p < 0.001$) ,respectively. At 24, 48 and 72 hours, cell viabilities for all subgroups of M2 macrophages were not significantly different from those of M0 control cells (Figure 6A, 7A, 8A). Compared to uninfected M1 macrophages at 24, 48 and 72hrs following cells polarization, uninfected IL-4, IL-10 and IL-13 induced M2 macrophages exhibited a significant increases in cell viability ($p<0.001$, $p<0.001$, and $p<0.001$, respectively).

Cell viabilities after HSV-1 infection

Following HSV-1 infection at 24, 48 and 72 hours of culture, no significant differences were seen in the viabilities of M1 macrophages (Figure 6B, 7B, 8B) as compared to control M0 cell. At 24 hours of

HSV-1 infection, M1 and all subgroups of M2 macrophages showed no significant cell viability changes compared to M0 cells.

In summary, similar to the observations of Reichard (2012) polarization appears to be the cause of decreases in cell viabilities of both infected and uninfected M1 macrophages compared with viabilities seen for M0 control cell and M2 macrophages polarized by IL-4, IL-10 or IL-13.

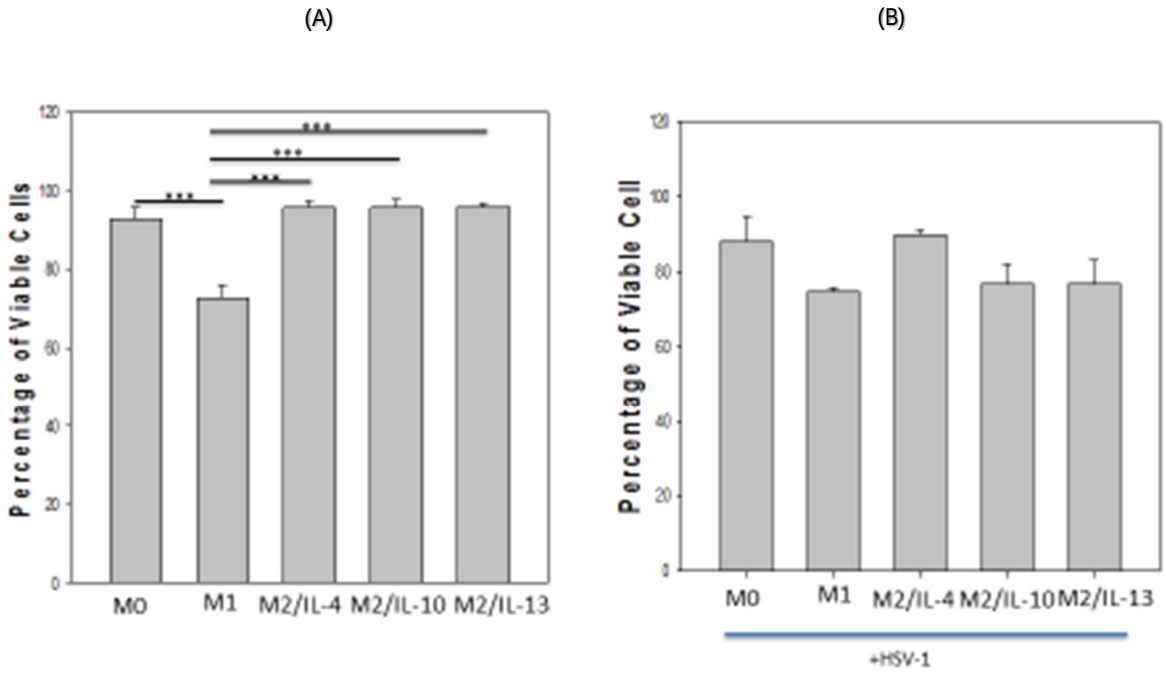

Figure 6: Cell viability of unpolarized (M0) and polarized macrophages (M1, M2) after 24 hours

(A) prior to HSV-1 infection; (B) after HSV-1 infection. Percentages of viable cells are shown as the mean and error bars represent standard error. One-way ANOVA with Tukey's post hoc test was applied. Black stars (*) indicate the significance level; ***, $p < 0.001$. (n= 3)

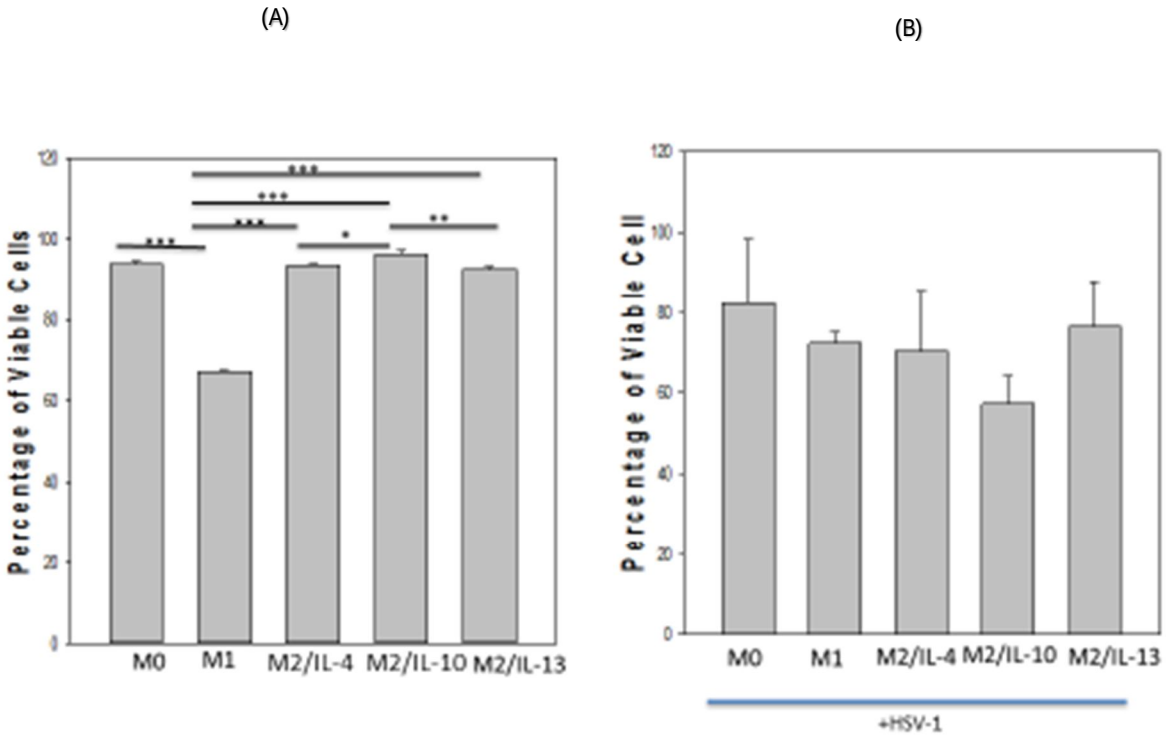

Figure 7: Cell viability of unpolarized (M0) and polarized macrophages (M1, M2) after 48 hours

(A) prior to HSV-1 infection; (B) after HSV-1 infection. Percentages of viable cells are shown as the mean and error bars represent standard error. One-way ANOVA with Tukey's post hoc test was applied. Black stars (*) indicate the significance level *, p <0.05; **, p< 0.010; ***, p <0.001. (n= 3)

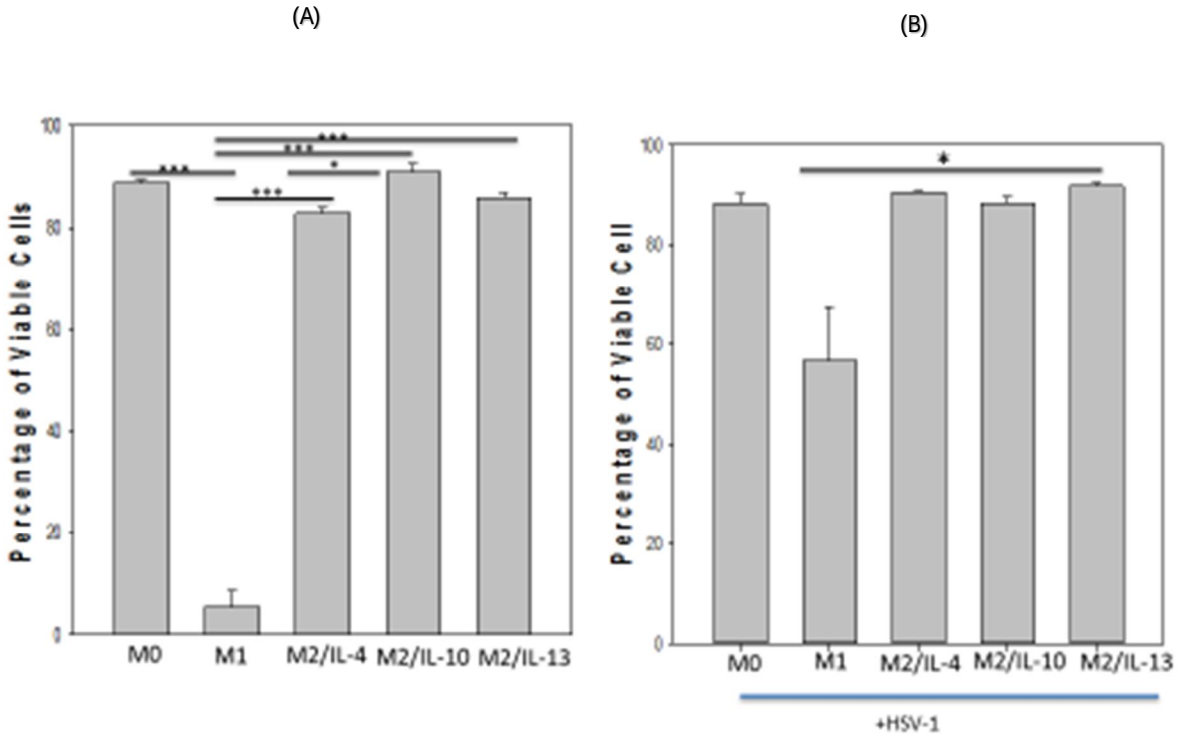

Figure 8: Cell viability of unpolarized (M0) and polarized macrophages (M1, M2) after 72 hours

(A) prior to HSV-1 infection; (B) after HSV-1 infection. Percentages of viable cells are shown as the mean and error bars represent standard error. One-way ANOVA with Tukey's post hoc test was applied. Black stars (*) indicate the significance level *, $p < 0.05$; **, $p < 0.010$; ***, $p < 0.001$. (n= 3)

Cell morphology

Morphological changes in absence and presence of the HSV-1 on polarized macrophages murine cells J774A.1 comparing to control Cells

Unpolarized M0 macrophages appeared mostly as rounded cells at 24, 48, and 72 hours of culture (Figure 9, 14). M1 macrophages polarized by treatment with IFN-γ and LPS for 24, 48, and 72 hours tend to appear flattened, enlarged, irregularly shaped, and vacuolated (as shown in Figure 9, 14). When compared to control cells, M2 macrophages polarized with IL-4 displayed both a rounded and an elongated cell morphology (Figure 9), whereas, M2 macrophages polarized with IL-10 or IL-13 exhibited mostly a rounded cell shape at 24, 48, and 72 hours (Figure 9). These morphological changes in either M1 or M2 macrophages might easily help to differentiate between the two phenotypes.

Following infection with HSV-1 (MOI 0.1), M0, M1 and M2 macrophages appeared smaller and exhibited similar rounded morphology for all (M1 and the subgroups of M2 macrophages) at 24, 48, and 72 hours (Figure 10, 15). When virus was not introduced into the culture, M1 macrophages showed different morphology compared to infected M1 macrophages. Uninfected M1 cells were flattened, enlarged, irregularly shaped, and vacuolated while infected M1 macrophages appeared rounded (Figure 9, 14).

Consequently, cells infected with HSV-1 virus showed similar morphological changes on M0, M1, or M2 macrophages; all cells became rounded which made it difficult to differentiate between M1 and M2 phenotypes based on morphology alone in HSV -1 infected cells (Figure 10, 15).

Immunofluorescent intensity-Tubulin

HSV-1-infected unpolarized and polarized J774A.1 cells were examined for fluorescent intensity of tubulin and F actin. Tubulin was detected by indirect immunofluorescence using rabbit polyclonal anti-αβ tubulin and FITC-labeled goat anti-rabbit globulin as the secondary antibody Texas Red-phalloidin was used to visualize polymerized actin (F-actin). Cells were observed using the Olympus inverted fluorescent microscope and two images were taken per field. Two different filters were used to take images: TRITC (tetramethylrhodamine, red) 500ms and FITC (Fluorescein isothiocyanate, green) 1900ms. The green (FITC) fluorescent intensity represents the level of tubulin staining, while the red (TRITC) fluorescent intensity represents the level of F-actin staining. ImageJ software was used to analyze the qualified region of interest (immunofluorescent) and to detect the relative cytoskeletal changes at 24, 48 and 72 hours with or without HSV-1 virus. All comparisons were significant by One-Way ANOVA. Comparisons between two groups were made using the T-test.

Analyses of uninfected versus infected unpolarized and polarized macrophages J774A.1

Tubulin intensity levels in uninfected and HSV-1-infected, unpolarized and polarized macrophages infection were evaluated by calculating the qualified region of interest (qROI) found by ImageJ divided by cell numbers on each image. Tubulin staining was significantly enhanced in HSV-1-infected unpolarized M0 cells as compared to uninfected M0 cells at 24 hour ($P<0.005$) (Figure 11). At this same time, HSV-1-infected M1 cells showed significantly less tubulin staining than did uninfected M1 cells ($p<0.001$). Unpolarized M2 cells induced by IL-10 showed a slight decrease in tubulin staining compared to uninfected M1 cells ($p<0.019$, NS). Significant differences in intensity of tubulin staining were not seen in the other macrophage subgroups examined.

After 48, HSV-1-infected polarized cells compared to their uninfected polarized counterpart showed decreases in tubulin staining but only the M1 and M2-IL-10 pairs showed significance ($p<0.01$) (Figure 12)

In contrast, tubulin staining was increased in the virus-infected cells remaining at 72 hours after polarization (Figure 13). Tubulin intensity was significantly increased in infected M1 and M2-IL-4 polarized cells ($p<0.001$).

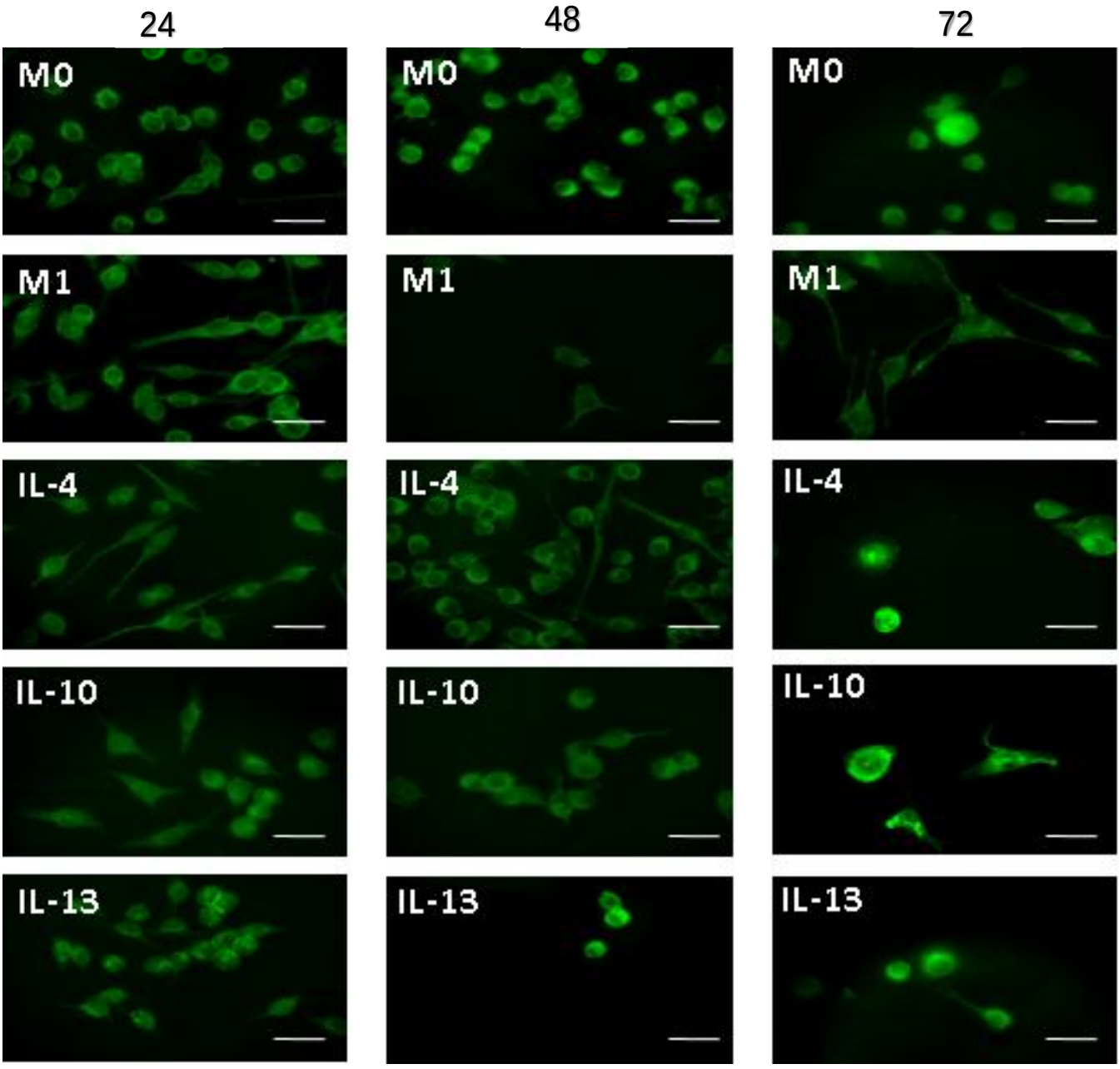

Figure 9: Tubulin immunofluorescent images of polarized and un-polarized J774A.1 macrophages cells show morphological changes and cytoskeleton immunostaining at 24, 48, and 72 hours prior to- HSV-1 infection.

Green fluorescence (FITC, tubulin) images show unpolarized and polarized macrophages that were fixed and stained with αβ-tubulin antibody for (microtubules arrangement) (Images captured at 60X oil magnification, scale bar =50μm) (n= 9).

M0 control unpolarized

M1 macrophages polarized by LPS and IFN-γ

M2 macrophages polarized by IL-4, IL-10, and IL-13 cytokines

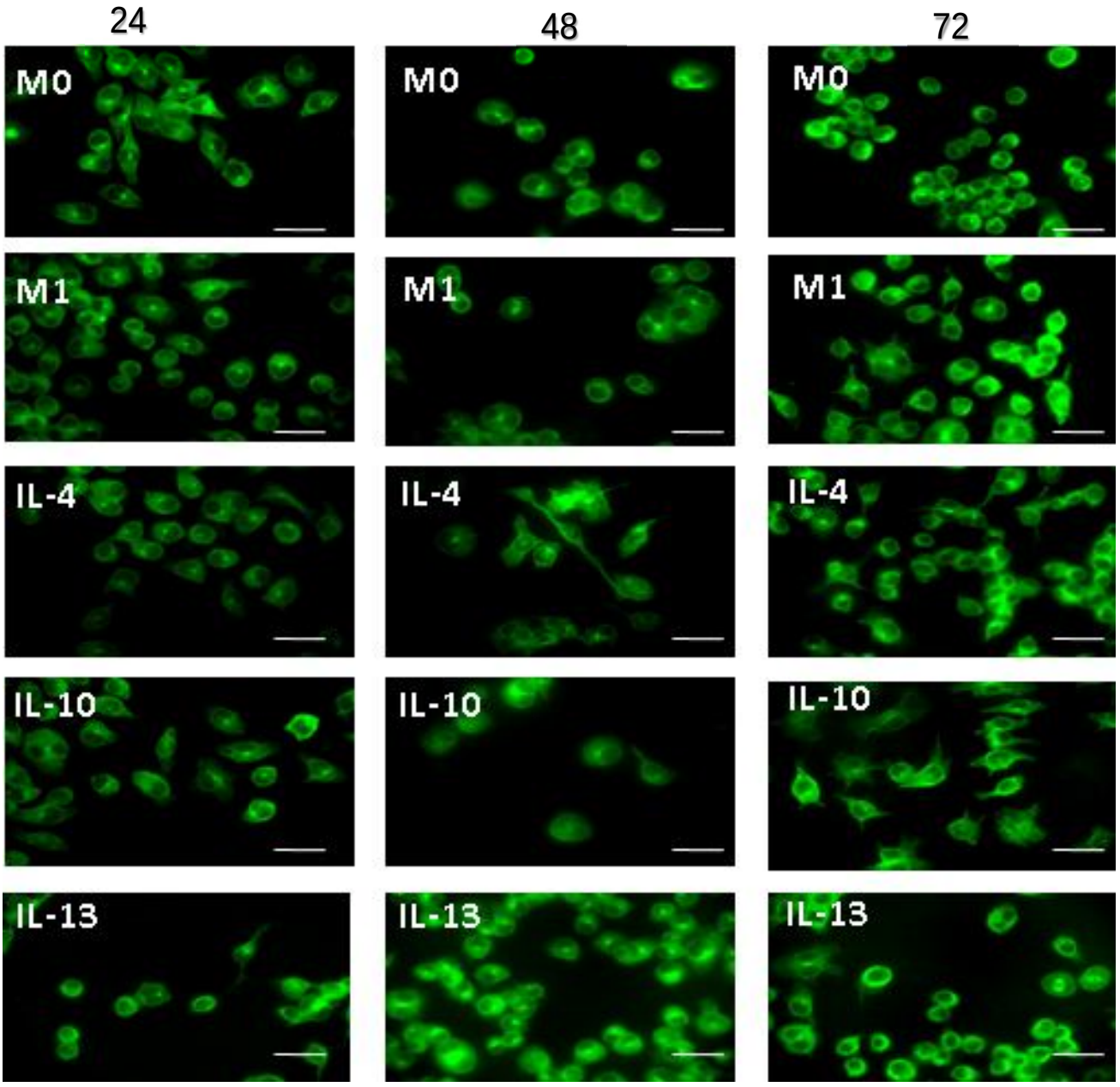

Figure 10: Tubulin immunofluorescent images of polarized and un-polarized J774A.1 macrophages cells show morphological changes and cytoskeleton immunostaining at 24, 48, and 72 hours after- HSV-1 infection.

Green fluorescence (FITC, tubulin) images show unpolarized and polarized macrophages that were fixed and stained with αβ-tubulin antibody for (microtubules arrangement) (Images captured at 60X oil magnification, scale bar =50µm) (n= 9).

M0 control unpolarized

M1 macrophages polarized by LPS and IFN-γ

M2 macrophages polarized by IL-4, IL-10, and IL-13 cytokines

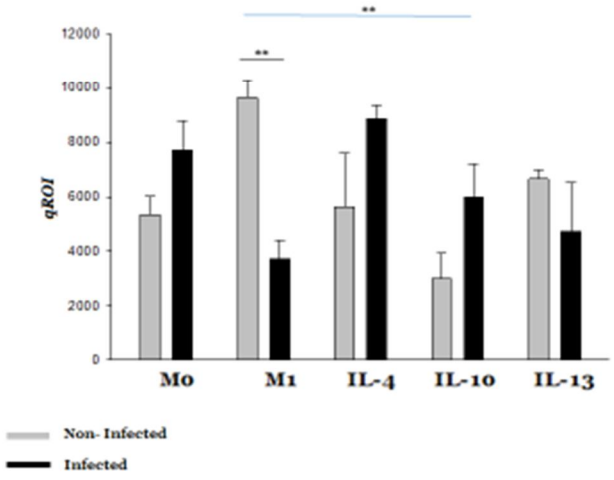

***Figure 11: Tubulin immunofluorescent intensity for control and polarized macrophages following 24 hours of cytokines prior to and after HSV-1 infection*.**

HSV-1 Infected cells (black bars) were compared to the uninfected cells (gray bars). *Black stars (*) indicate the significance level; **, p <0.01.*

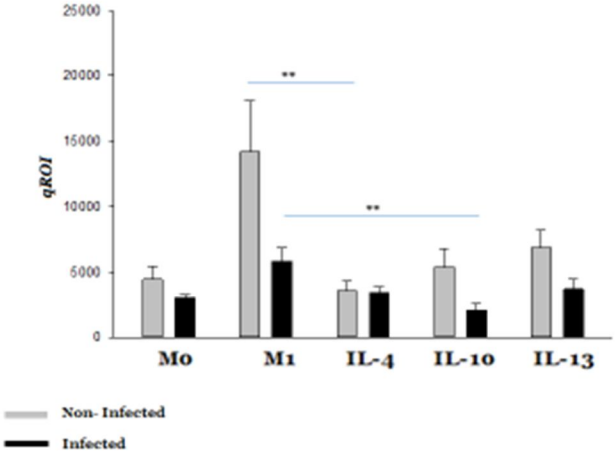

***Figure 12: Tubulin immunofluorescent intensity for control and polarized macrophages following 48 hours of* cytokines prior to and after HSV-1 infection.**

HSV-1 Infected cells (black bars) were compared to the un-infected cells (gray bars). Black stars (*) indicate the significance level; **, $p < 0.01$.

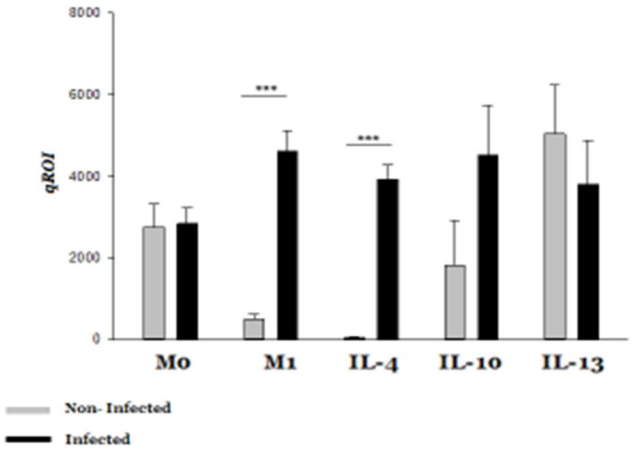

Figure 13: Tubulin immunofluorescent intensity for control and polarized macrophages following 72 hours of cytokines prior to and after HSV-1 infection.

HSV-1 Infected cells (black bars) were compared to the un-infected cells (gray bars). Black stars (*) indicate the significance level; ***, $p < 0.001$.

Immunofluorescent intensity-F-Actin

Analyses of uninfected versus infected unpolarized and polarized macrophages J774A.1

All comparisons were significant by One-Way ANOVA. Comparisons between two groups were made using the T-test. F-actin intensity levels in uninfected and HSV-1-infected, unpolarized and polarized macrophages infection was evaluated by calculating the qualified region of interest (qROI) divided by cells number on each image. As shown in Figure 16 at 24 hours after polarization, virus-infected cells exhibited greater amounts of F-actin staining except for the M1 polarized and M2-1L-13 polarized cells in which equal intensities of F-actin were seen for both the infected and uninfected polarized cells. Significant increases in F-actin expression occurred in virus-infected M0 ($p<0.005$) and IL-10-polarized cells ($p<0.01$) over their uninfected counterparts. At 48 hours (Figure 17), virus-infected macrophage subgroups exhibited less fluorescence than the uninfected unpolarized or polarized macrophages. Significance was seen ($P<0.0$) in M1 versus M1-infected cells. By 72 hours (Figure 18), all-infected cultures, unpolarized or polarized, showed considerably less F-actin staining. All M2 groups showed significant decreases in F-actin expression by HSV-1-infected cells with M2 cells polarized with IL-4 cells showing the most ($p<0.005$); M2 cells polarized with IL-10 or IL-13 showed significances of ($p<0.01$).

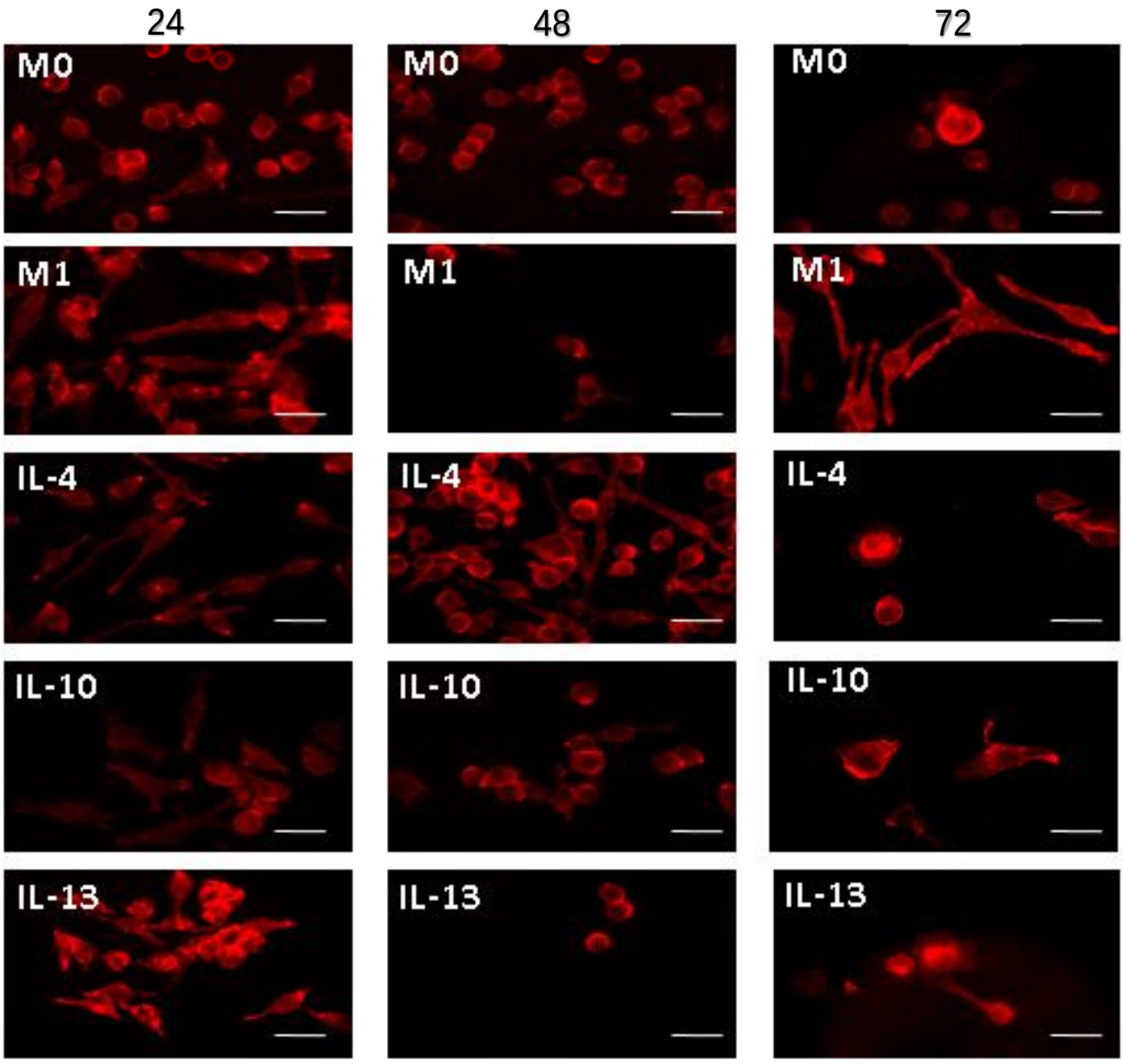

Figure 14: F-actin immunofluorescent images of polarized and un-polarized J774A.1 macrophages cells show morphological changes and cytoskeleton immunostaining at 24, 48, and 72 hours prior to- HSV-1 infection.

Red fluorescence (TRITC, F-actin) images show phalloidin (for filamentous actin arrangement) (Images captured at 60X oil magnification, scale bar =50µm) (n= 9).

M0 control unpolarized

M1 macrophages polarized by LPS and IFN-γ

M2 macrophages polarized by IL-4, IL-10, and IL-13 cytokines

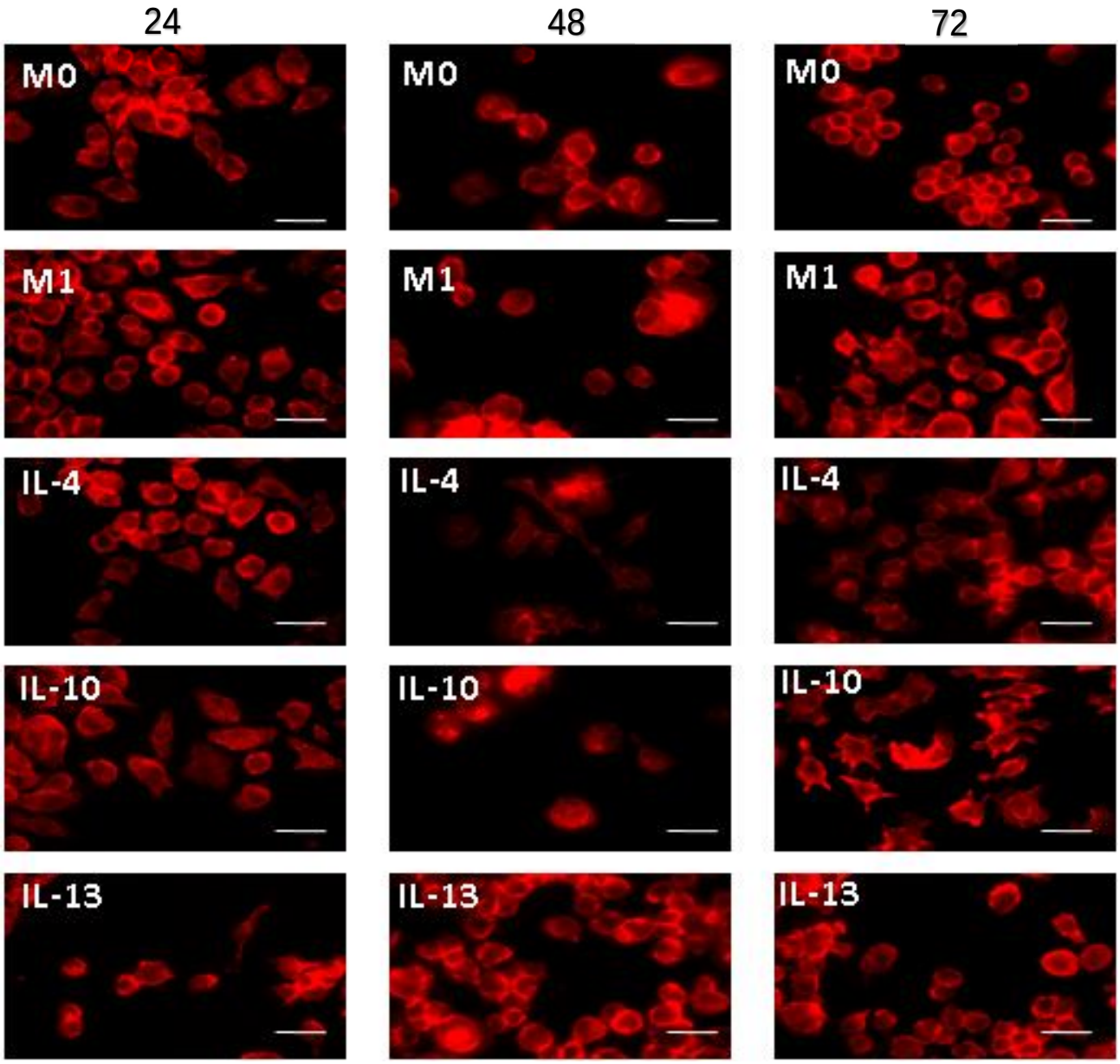

Figure 15: F-actin immunofluorescent images of polarized and un-polarized J774A.1 macrophages cells show morphological changes and cytoskeleton immunostaining at 24, 48, and 72 hours after to- HSV-1 infection.

Red fluorescence (TRITC, F-actin) images show phalloidin (for filamentous actin arrangement) (Images captured at 60X oil magnification, scale bar =50µm) (n= 9).

M0 control unpolarized

M1 macrophages polarized by LPS and IFN-γ

M2 macrophages polarized by IL-4, IL-10, and IL-13 cytokines

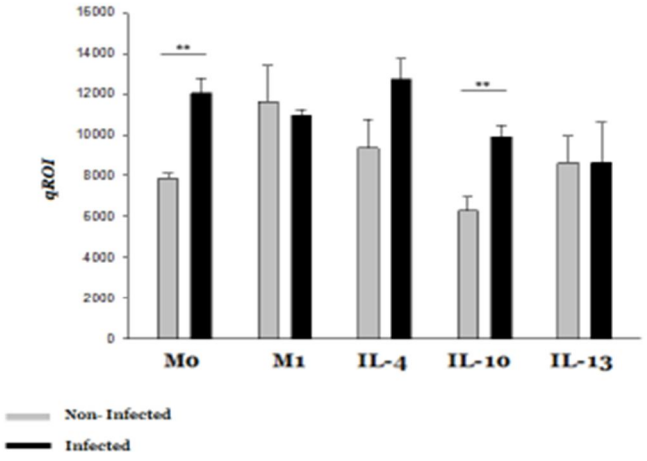

Figure 16: F-actin immunofluorescent intensity for control and polarized macrophages following 24 hours of cytokines prior to and after HSV-1 infection.

HSV-1 Infected cells (black bars) were compared to the uninfected cells (gray bars). Black stars (*) indicate the significance level; **, $p < 0.01$.

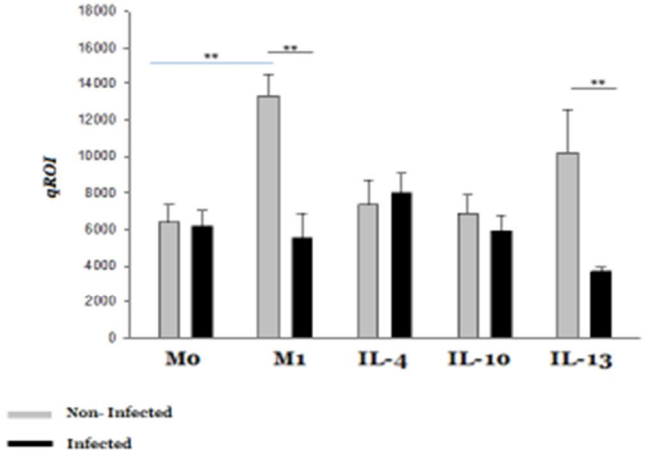

Figure 17: F-actin immunofluorescent intensity for control and polarized macrophages following 48 hours of cytokines prior to- and after-HSV-1 infection.

HSV-1 Infected cells (black bars) were compared to the un-infected cells (gray bars). Black stars (*) indicate the significance level; **, $p < 0.01$.

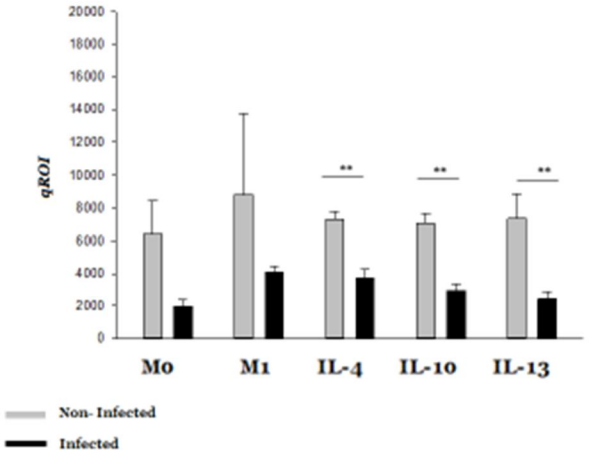

Figure 18: F-actin immunofluorescent intensity for control and polarized macrophages following 72 hours of cytokines prior to- and after-HSV-1 infection.

HSV-1 Infected cells (black bars) were compared to the un-infected cells (gray bars). Black stars (*) indicate the significance level; **, $p < 0.01$.

DISCUSSION

The first host response to HSV-1 infection is mediated by the innate response involving macrophages and natural killer cells. Macrophages cell can direct the host immune system to produce specific pro- and anti-inflammatory cytokines that cause alterations in cellular homeostasis and inhibit virus replication. In phagocytosis by macrophages, HSV-1 is eliminated by reactive oxygen species (ROS), nitric oxide (NO), and cytotoxins such as tumor necrosis factor-alpha (TNF-α). This study indicates that unpolarized or polarized HSV-1-infected M1 inflammatory macrophages exhibited significant reductions in the cell viability compared to unpolarized M0 control cell and M2 anti-inflammatory macrophages polarized by IL-4, IL-10 and IL-13. This reduction in cell viability was expected due to the crucial role of macrophages play in viral clearance and has been seen previously in J774A.1 in our laboratory by Reichard (2012). This finding agreed with the literature that the decrease in M1 macrophage cell viability is due to secreted pro-inflammatory products such as IFN-γ/TNF-α which together are known to be toxic to the cell and lead to cell death. (Wang *et al.,* 2011).

Immunofluorescence images showed that uninfected M1 cells were flattened, irregularly shaped, and contained visible intracellular vacuoles compared to rounded cell shape exhibited in uninfected M0 or M2 polarized macrophages. Uninfected M2 macrophages stimulated by IL-4 showed a combination of morphologies ranging from elongated to rounded cells. Furthermore, uninfected M2 macrophages stimulated by IL-10 or IL-13 displayed a rounded cell type which closely resembled unpolarized (M0) cells.

Following HSV-1 infection, all macrophage subgroups (M0, M1, and the three M2 phenotypes) were indistinguishable, showing smaller rounded cell morphologies. These observations are consistent

with the study of Taylor *et al.* (2011) that during virus infection, viral proteins cause drastic changes and rearrangement of the cellular actin and cell signaling during virus proliferation. The most prominent changes in cell morphology caused by many viruses including HSV-1 is rounded cell shape. These morphological changes are likely a result of alterations in the actin cytoskeleton rearrangements that occur during the normal virus life cycle (Bigley, 2014; Reichard, 2012).

In addition to F-actin, the tubulin filaments were analyzed in this study. The relative amounts of the tubulin and F-actin microfilaments were evaluated by determining the fluorescent intensity of immunofluorescent microscopy images and quantifying through Image J analysis. The main goal of this study was to determine the cytoskeleton changes during HSV-1 infection of unpolarized and polarized cells using indirect immunofluorescence. It is well established that HSV-1 depends heavily on the cell cytoskeleton for its replication cycle and intracellular trafficking (Turowska *et al.,* 2010; Campbell et. al., 2005). During a study of the effects of varicella-zoster virus infection on the cytoskeletal components (actin, lamin A, tubulin and vimentin), Kuhn and colleagues (2005) observed that the amounts of actin, tubulin and vimentin start to decrease continuously from 24 hours to 48 hours post infection until the end of the viral cycle replication.

Similarly, in this present study, the majority of uninfected M1 and M2 macrophages subgroups displayed increased levels of tubulin and F-actin compared to uninfected M0 control cells. In contrast, infection by HSV-1 markedly reduced the immunofluorescent intensity of either tubulin or F-actin 48 hours after polarization and infection of M1 and M2. By 72 hours, the opposite was seen in that greater amounts of tubulin and F-actin were present in all polarized and infected cells (M0, M1, and the three M2 phenotypes). One explanation for this phenomenon might be that the viable cells remaining culture were involved in replicating virus and preventing apoptosis of the cells in

cultures. Evidence to support this contention comes from Roizman and Taddeo (2007) who describe ways in which HSV blocks pro-apoptotic cellular functions. More recently, Aubert *et al.,* (2008) observed that the antiapoptotic herpes simplex virus glycoprotein J localizes to multiple cellular organelles.

Mcwhorter et al., (2013) found that uninfected M2 macrophages polarized with IL-4 or IL-13 displayed higher F-actin fluorescence levels compared to uninfected, unstimulated cells or M1 macrophages polarized with LPS/IFN-γ. They determined that the actin cytoskeleton is an important factor of shape-induced macrophage polarization. Interestingly, in this study uninfected M1 and M2 polarized macrophages induced by IL-10 and IL-13 showed increased levels of F-actin by 24 and 48 hours.

In the present study, HSV-1 infected M1 and M2 macrophages polarized by IL-10 or IL-13 showed reduced levels of F-actin by 24 and 48 hours while comparable cell populations of infected cells at 72 hours showed up-regulation of the F actin levels These observations agree with those of Lyman and Enquist (2008) who found that the cell microfilaments disassembled to at 4 hours after HSV-1 infection with a continuous decrease in F-actin occurring over the next 12 to 16 hours in a Vero cell model. In another study, Xiang and his colleagues (2012) used neuronal cells to investigate the role of F-actin in HSV-1 infection and replication. They found that HSV-1 infection enhances F-actin assembly during the primary stage of infection, while F-actin levels decrease at later stages of infection in the cell. They suggested that F-actin assembly enhanced during the early phases of HSV-1 infection would benefit the intracellular viral transport. Moreover, HSV-1 infection caused a continuous decrease in cellular F-actin levels during the later stages of infection in favor of viral

reproduction at later stages of infection as replication (Xiang *et al.*, 2012). HSV-1 induces changes in F-actin cytoskeleton of infected cells for its benefit during the infection process.

FUTURE STUDIES

In future studies, it would be beneficial to study the effects on viability and cytoskeleton filaments on freshly isolated primary macrophages at these same times as well as at 2, 4, 6, 10, and 12 intervals prior to and after HSV-1infection to see the effects of the early stages of virus replication starting from virus glycoproteins binding to cell surface receptors.

It would be of interest to determine whether anti-apoptotic effects are actually occurring in the virus-infected cultures in later stages of infection of the polarized cells e.g. at 72 hours. For example, this could be determined by looking for evidence of apoptosis-anti apoptosis-by staining of cells for annexin V, and use of the tunnel assay. There are commercially available kits to measure apoptosis.

It is difficult to explain that tubulin levels are markedly increased while F-actin levels are decreased by 72 hour after HSV-1 infection in the image analyses experiment. In each of these, only the least background noise 3 images were analyzed per treatment. To verify these observations, repeating the experiments using confocal microscopy to analyze image fluorescent intensity would be helpful.

This study measured only polymerized F-actin after staining with Texas Red-Phalloidin X. Once Phalloidin binds to F-actin, it prevents the depolymerization of the actin fibers. So, it is important for further studies to use an analytical technique like western blot to detect both monomeric and polymeric filaments (F-actin + G-actin). There are many companies that specialize in providing the suitable antibodies against monomer G-actin and polymer F-actin. So, detection of the overall pools of actin protein levels (polymerized and depolymerized actin) will give a better understanding of the viral effects in microfilaments cell cytoskeleton.

Since virus replication depends on egress from infected cells shuttled to the cell surface via microtubule transport, it would be of interest to determine virus yield (pfu assays) per number of cells/well at 24, 48 and 72 hours after HSV-1 infection. Reichard, Cheemarla, and Bigley (2015) noted that 4 fold less virus was produced in J774A.1 M1-polarized cells than in M0 cells at 24 hours after HSV-1 infection. M1 cells demonstrated a 2.5-fold reduction in virus pfu by comparison with infected M2 cells. These observations suggested that lower virus titers were released from M1-polarized cells because the polarization process was killing the cells and there were fewer cell with what the virus could replicate. This phenomenon was not unique to the J774A.1 macrophages since M1-polarized RAW264.7 macrophages yielded 3-fold less virus at 24 hours after infection than did infected and unpolarized M0 RAW264.7 cells or infected M2-polarized RAW264.7 cells.

REFERENCES

Aubert, M., Chen, Z., Lang, R., Dang, C. H., Fowler, C., Sloan, D. D., and Jerome, K. R. 2007. The Antiapoptotic Herpes Simplex Virus Glycoprotein J Localizes to Multiple Cellular Organelles and Induces Reactive Oxygen Species Formation. J. Virol. 82: 617629.

Barois N, Forquet F, Davoust J. 1998. Actin microfilaments control the MHC class II antigen Presentation pathway in B cells. J. Cell Sci. 111:1791–800.

Bigley, N. J. 2014. Complexity of Interferon-γ Interactions with HSV-1. Front. Immunol. 5(15):1-9**.**

Campbell, E. M., and Hope, T. J. 2005. Gene Therapy Progress and Prospects: Viral trafficking During infection. Gene Ther. 12:1353-1359.

Casrouge, A., Zhang, S., Eidenschenk, C., Jouanguy, E., Puel, A., Yang, K., and Casanova, J.2006. Herpes Simplex Virus Encephalitis in Human UNC-93B Deficiency. Science, 314(5797), 308-312.

Clement, C., Tiwari, V., Scanlan, P. M., Valyi-Nagy, T., Yue, B. Y., and Shukla, D. 2006. A Novel role for phagocytosis-like uptake in herpes simplex virus entry. J. Cell Biol. 174: 1009-1021.

Davis, M. J., Tsang, T. M., Qiu, Y., Dayrit, J. K., Freij, J. B., Huffnagle, G. B., and Olszewski, M.**A**. 2013. Macrophage M1/M2 Polarization Dynamically Adapts to Changes in Cytokine Microenvironments in Cryptococcus neoformans Infection. MBio 4(3).

Favoreel, H. W., Enquist, L., and Feierbach, B. 2007. Actin and Rho GTPases in herpesvirus Biology. Trends Microbiol.15: 426-433.

Frampton, A. R., Goins, W. F., Nakano, K., Burton, E. A., and Glorioso, J. C. 2005. HSV trafficking and development of gene therapy vectors with applications in the nervous system. Gene Ther. 11: 891-901.

Frausto-Del-Río, D., Soto-Cruz, I., Garay-Canales, C., Ambriz, X., Soldevila, G., Carretero-Ortega, J.and Ortega, E. 2012. Interferon gamma induces actin polymerization, Rac1 activation and down regulates phagocytosis in human monocytic cells. Cytokine 57: 158-168.

Gabhann, J. N., Hams, E., Smith, S., Wynne, C., Byrne, J. C., Brennan, K., and Jefferies, C. A. 2014. Btk Regulates Macrophage Polarization in Response to Lipopolysaccharide. PLoS ONE 9:1-11.

Geraghty, R. J., Krummenacher, C., Cohen, G. H., Eisenberg, R. J, Spear, P.G. 1998. Entry ofAlphaherpesviruses Mediated by Poliovirus Receptor-Related Protein 1 and Poliovirus Receptor. Science, 280(5369):1618-1620.

Hu, Y., Hu, X., Boumsell, L., and Ivashkiv, L. B. 2008. IFN- and STAT1 Arrest Monocyte Migration and Modulate RAC/CDC42 Pathways. J. Immunol.180: 8057-8065.

Huang, W., Su, Y., Yao, H., Ling, P., Tung, Y., Chen, S., and Chen, S. 2009. Beta interferon plus gamma interferon efficiently reduces acyclovir-resistant herpes simplex virus infection in mice in a T-cell-independent manner. J. Gen. Virol. 91: 591-598.

Johnson, H., Noon-Song, E., Kemppainen, K., and Ahmed, C. 2012. Steroid-like signalling by interferons: making sense of specific gene activation by cytokines. Biochem. J. 443: 329-338.

Karasneh, G. A., and Shukla, D. 2011. Herpes simplex virus infects most cell types in vitro: Clues to its success. Virol. J. 8: 481(1-11).

Kuhn, M., Desloges, N., Rahaus, M., and Wolff, M. H. 2005. Varicella-Zoster Virus Infection Influences Expression and Organization of Actin and α-Tubulin but Does Not Affect Lamin A and Vimentin. Intervirol. 48:312-320.

Lyman, M. G., and Enquist, L. W. 2008. Herpesvirus Interactions with the Host Cytoskeleton. J. Virol. 83: 2058-2066.

Martinez, F. O., Sica, A., Mantovani, A. and Locati, M. 2008. Macrophage activation and polarization. Front. Biosci. 13: 453-461.

Mcwhorter, F. Y., Wang, T., Nguyen, P., Chung, T., & Liu, W. F. 2013. Modulation of macrophage phenotype by cell shape. Proc. Nat. Acad. Sci. USA. 110(43), 17253-17258.

Mosser, D. M., and Edwards, J. P. 2010. Exploring the full spectrum of macrophage activation. Nat. Rev. Immunol. 10: 460-460.

Martinez, F. O., and Gordon, S. 2014. The M1 and M2 paradigm of macrophage activation: Time for reassessment. F1000 Prime Rep. 6:1-13.

Otth, C., Zambrano, A., & Concha, M. 2009. The Possible Link between Herpes Simplex Virus Type 1 Infection and Neurodegeneration. In Current Hypotheses and Research Milestones in Alzheimer's Disease, pages 181-188. R.B. Maccioni and G. Perry (ed)

Parker, A. L., Kavallaris, M., and Mccarroll, J. A. 2014. Microtubules and Their Role in Cellular Stress in Cancer. Front. Oncol. 4:38-43.

Quinn, M., Mcmillin, M., Frampton, G., Humayra, S., Huang, L., and Demorrow, S.2012. The Role of the Tumor Microenvironment in the Pathogenesis of Cholangiocarcinoma.

Pages 59-74 in Liver Tumors. A. Julianov (ed).Publisher INTECH.

Rahn, E., Petermann, P., Hsu, M., Rixon, F. J., and Knebel-Mörsdorf, D. 2011. Entry Pathways of Herpes Simplex Virus Type 1 into Human Keratinocytes Are Dynamin- and Cholesterol-Dependent. PLoS ONE, 6(10): 1-13.

Reichard, A. 2012. The effects of HSV-1Chllenge on polarized Murine Macrophages: an in Vitro Mouse Using the J774A.1 Murine Macrophage Cell Line. Ohio Link., p70.

Reichard, A.C., Cheemarla, N.R., and Bigley, N.J. 2015. SOCS1/3 Expression Levels in HSV 1-Infected, Cytokine-Polarized and -Unpolarized Macrophages. J. Interf. Cytok. Res. 35: 32-41.

Roberts, K. L., and Baines, J. D. 2011. Actin in Herpesvirus Infection. Viruses 3:336-346.

Roizman B., and Taddeo B. 2007. The strategy of herpes simplex virus replication takeover of the host cell. (Chapter 13) In Human Herpesviruses: Biology, Therapy, and Immunopropholaxis. Arvin A, Campbell-Fiume G, Mocarski E, et al. (eds).

Sodeik, B., Ebersold, M. W., and Helenius, A. 1997. Microtubule-mediated Transport of Incoming Herpes Simplex Virus 1 Capsids to the Nucleus. J. Cell Biol. 136:1007-1021.

Spear, M., and Wu, Y. 2014. Viral exploitation of actin: force-generation and scaffolding functions in viral infection. Virol. Sin. 29:139-147.

Stefater, J. A., Ren, S., Lang, R. A., and Duffield, J. S. 2011. Metchnikoff's policemen: macrophages in development, homeostasis and regeneration. Trend. Mol. Med. 17:743-752.

Stöger, J. L., Gijbels, M. J., Velden, S. V., Manca, M., Loos, C. M., Biessen, E. A., and Winther, P. 2012. Distribution of macrophage polarization markers in human atherosclerosis. Atheroscler. 225:461-468.

Sum, M. S. 2015. The Involvement of Microtubules and Actin during the Infection of Japanese Encephalitis Virus in Neuroblastoma Cell Line, IMR32. BioMed. Res. Internat. 2015:1-8.

Taylor, M. P., Koyuncu, O. O., and Enquist, L. W. 2011. Subversion of the actin cytoskeleton during viral infection. Nat. Rev. Micro. 9:427-439.

Turowska, A., Pajak, B., Godlewski, M. M., Dzieciątkowski, T., Chmielewska, A., Tucholska, A., and Banbura, M. 2010. Opposite effects of two different strains of equine herpesvirus 1 infection on cytoskeleton composition in equine dermal ED and African green monkey kidney Vero cell lines: Application of scanning cytometry and confocal-microscopy-based image analysis in a quantitative study. Arch. Virol. 155:733-743.

Wakimoto, H., Johnson, P. R., Knipe, D. M., and Chiocca, E. A. 2003. Effects of innate

immunity on herpes simplex virus and its ability to kill tumor cells. Gene Ther, 10:983-990.

Wang, N., Liang, H., and Zen, K. 2014. Molecular Mechanisms That Influence the Macrophage M2 Polarization Balance. Front. Immunol.5:230-238.

Xiang, Y., Zheng, K., Ju, H., Wang, S., Pei, Y., Ding, W.and Wang, Y. 2012. Cofilin 1 Mediated Biphasic F-Actin Dynamics of Neuronal Cells Affect Herpes Simplex Virus Infection and Replication. J. Virol. 86: 8440-8451.

Xu, L., Yang, F., Lin, R., Han, C., Liu, J., and Ding, Z. 2014. Induction of M2 Polarization in Primary Culture Liver Macrophages from Rats with Acute Pancreatitis. PLoS ONE, 9:1-8.

Zaichick, S., Bohannon, K., and Smith, G. 2011. Alphaherpesviruses and the Cytoskeleton in Neuronal Infections. Viruses 3:941-981.

APPENDIX

Table 2: Summary of the immunofluorescent intensity levels of tubulin on the un-polarized and polarized macrophages prior to- and after- HSV-1 infection

	-HSV-1 or +HSV-1	M0	M1	M2/IL-4	M2/IL-10	M2/IL-13
After 24 hrs. of treatments	-HSV-1	mean of qROI =5345.537	= 9627.838 Increased (P = 0.018)	=5635.769 No difference	= 3018.102 Reduced (P = 0.018)	= 6651.782 Slightly increased (P = 0.018)
	+HSV-1	mean of qROI =7709.171	= 3746.243 NS reduced	=8857.90 NS minor increased	= 5995.768 NS Reduced	= 4727.157 NS Reduced
	HSV-1 infected cells compared to uninfected	Increased (P = 0.007)	Reduced (P = 0.003)	NS increased	NS increased	NS reduced
After 48 hrs. of treatments	-HSV-1	mean of qROI =4464.859	=14176.528 Increased (P = 0.026)	=3625.901 Slightly reduced (P = 0.026)	=5413.647 Slightly increased (P = 0.026)	=6880.747 Minor increased (P = 0.026)
	+HSV-1	mean of qROI =3042.720	=5866.068 Increased (P = 0.023)	=3490.905 No difference (P = 0.023)	=2081.367 Reduced (P = 0.023)	=3727.713 Increased (P = 0.023)
	HSV-1 infected cells compared to uninfected	NS slightly reduced	NS greatly reduced	No difference	Reduced	Reduced
After 72 hrs. of treatments	-HSV-1	mean of qROI =2765.690	487.012 Greatly reduced (P = 0.007)	52.607 Greatly reduced (P = 0.007)	1828.078 Reduced (P = 0.007)	5039.210 Increased (P = 0.007)
	+HSV-1	mean of qROI =3213.526	5039.346 NS Increased	4232.950 NS increased	3458.976 NS slight increased	2848.509 NS slight reduced
	HSV-1 infected cells compared to uninfected	NS slightly increased	Greatly increased (P = <0.001)	Greatly increased (P= <0.001)	NS greatly increased	NS reduced

* NS: Non Significant

Table 3: Summary of the immunofluorescent intensity levels of F-actin on the un-polarized and polarized macrophages prior to- and after- HSV-1 infection

	-HSV-1 or +HSV-1	M0	M1	M2/IL-4	M2/IL-10	M2/IL-13
After 24 hrs. of treatments	-HSV-1	mean of qROI =7861.826	=11622.038g NS greatly increased	=9348.029 NS greatly increased	=6284.314 NS minor reduced	=8627.542 NS increased
	+HSV-1	mean of qROI =12011.561	=10928.939 NS reduced	=12699.794 No difference	=9901.761 NS reduced	=8639.990 NS reduced
	HSV-1 infected cells compared to uninfected	greatly increased (P = 0.006)	No difference	NS increased	increased (P = 0.015)	No difference
After 48 hrs. of treatments	-HSV-1	mean of qROI =6408.197	=13321.639 Greatly increased (P = 0.030)	=7379.757 Increased (P = 0.035)	=6862.626 Increased (P = 0.035)	=10218.135 Greatly increased (P = 0.035)
	+HSV-1	mean of qROI =6196.566	=5512.156 NS slightly reduced	=8006.440 NS increased	=5918.863 NS slightly reduced	=3696.478 NS reduced
	HSV-1 infected cells compared to uninfected	No difference	Greatly reduced (P = 0.012)	No difference	No difference	Greatly reduced (P = 0.049)
After 72 hrs. of treatments	-HSV-1	mean of qROI =5014.519	=8962.147 NS increased	=6872.022 No difference	=6665.923 No difference	=6647.800 No difference
	+HSV-1	mean of qROI =1942.651	=4087.035 Greatly increased (P = 0.032)	=3734.066 Greatly increased (P = 0.032)	=2983.226 Increased (P = 0.032)	=2397.919 Increased (P = 0.032)
	HSV-1 infected cells compared to uninfected	Greatly reduced	Greatly reduced	Greatly reduced (P = 0.008)	Greatly reduced (P = 0.004).	Greatly reduced (P = 0.038)

* NS: Non Significant

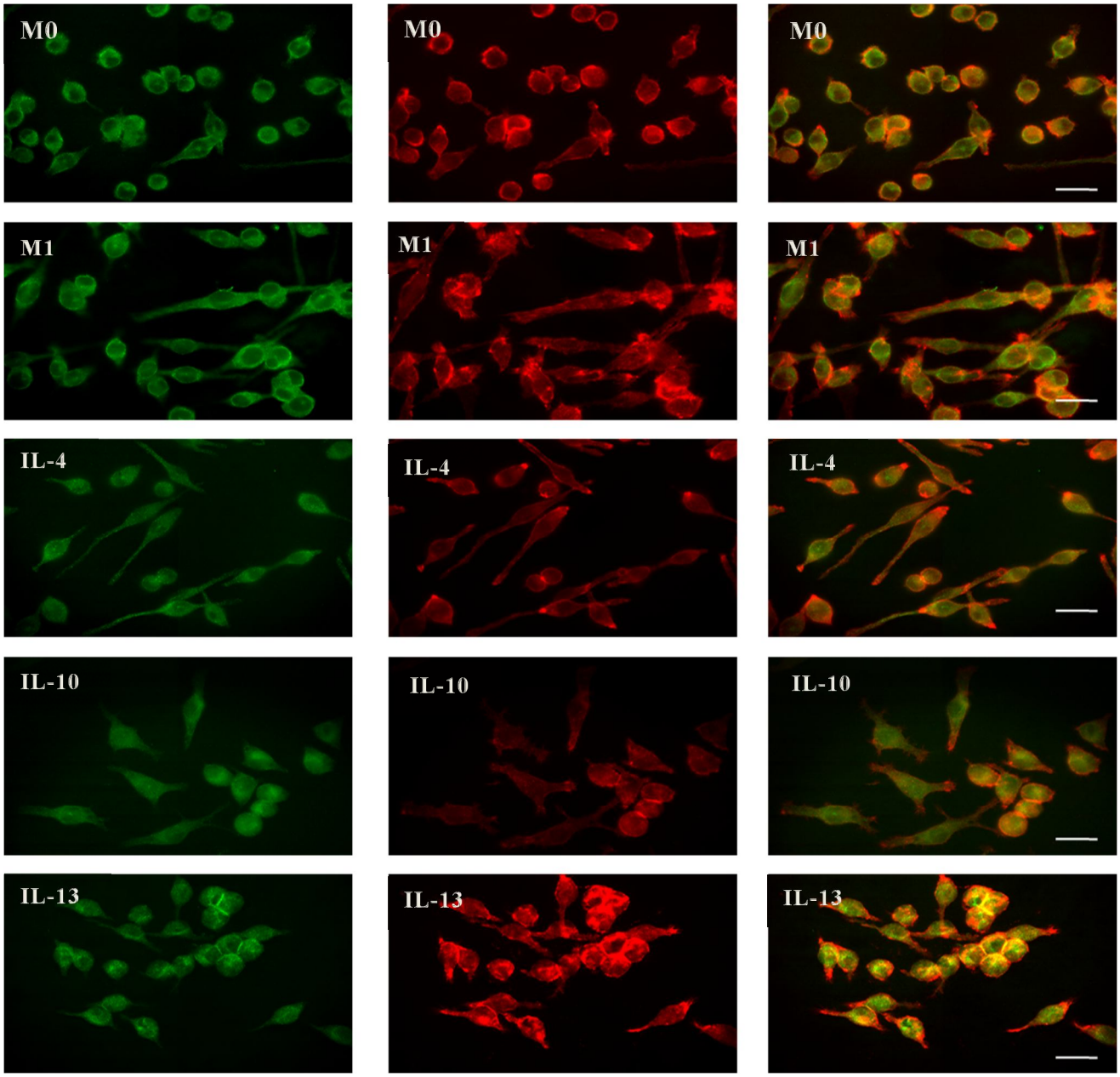

Figure 19: Immunofluorescent images of polarized and un-polarized J774A.1 macrophages cells show morphological changes and cytoskeleton immunostaining at 24 hours prior to- HSV-1 infection.

Green fluorescence (FITC, tubulin) images show unpolarized and polarized macrophages that were fixed and stained with αβ-tubulin antibody for (microtubules arrangement) in the first Colum, red fluorescence (TRITC, F-actin) images show phalloidin (for filamentous actin arrangement) in the second Colum, and the last Colum show the overlay between tubulin and phalloidin staining (Images captured at 60X oil magnification, scale bar =50μm) (n= 9).

M0 control unpolarized

M1 macrophages polarized by LPS and IFN-γ

M2 macrophages polarized by IL-4, IL-10, and IL-13 cytokines

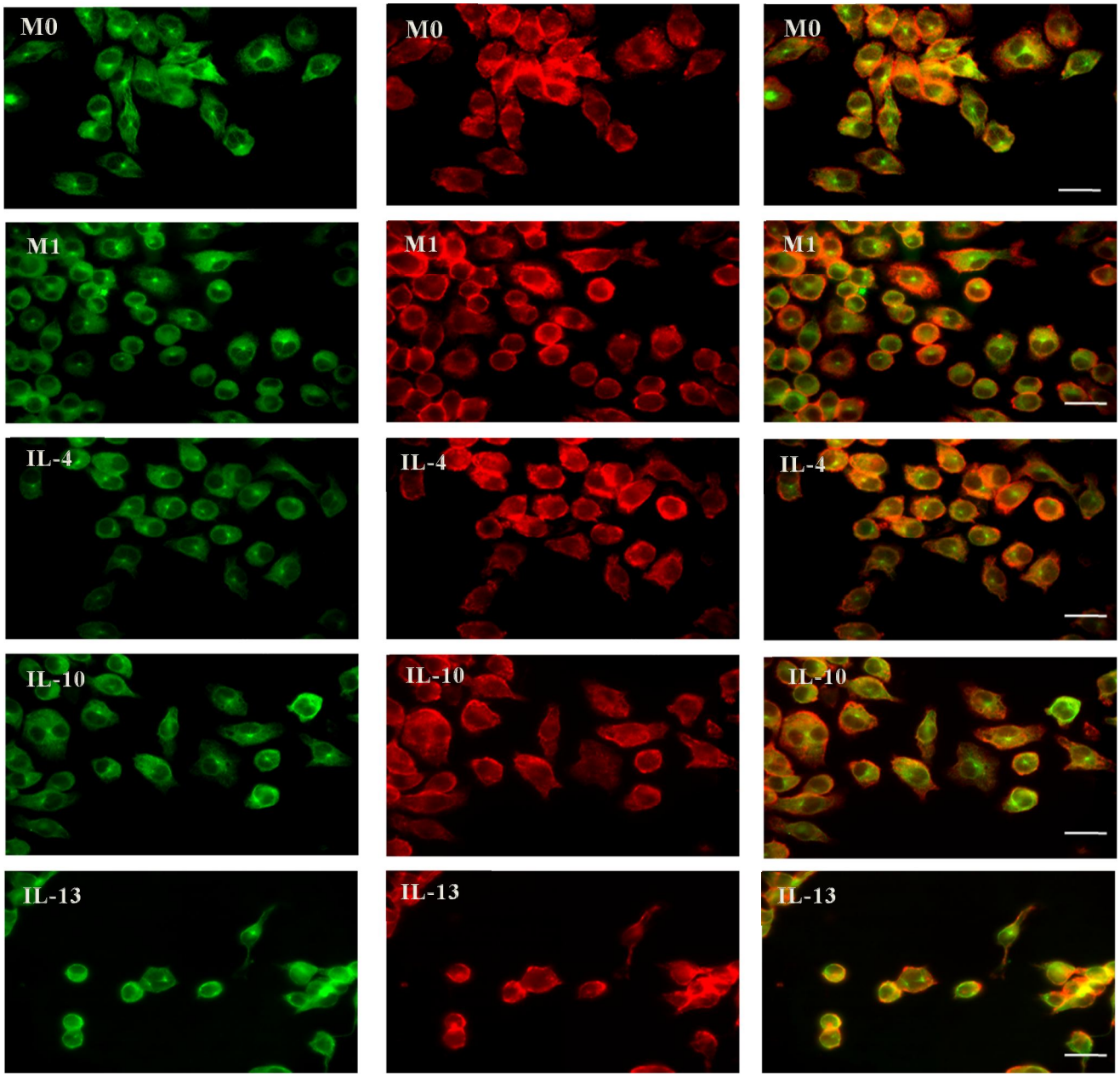

Figure 20: Immunofluorescent images of polarized and un-polarized J774A.1 macrophages cells show morphological changes and cytoskeleton immunostaining at 24 hours after- HSV-1 infection.

Green fluorescence (FITC, tubulin) images show unpolarized and polarized macrophages that were fixed and stained with αβ-tubulin antibody for (microtubules arrangement) in the first Colum, red fluorescence (TRITC, F-actin) images show phalloidin (for filamentous actin arrangement) in the second Colum, and the last Colum show the overlay between tubulin and phalloidin staining (Images captured at 60X oil magnification, scale bar =50μm) (n= 9).

M0 control unpolarized

M1 macrophages polarized by LPS and IFN-γ

M2 macrophages polarized by IL-4, IL-10, and IL-13 cytokines

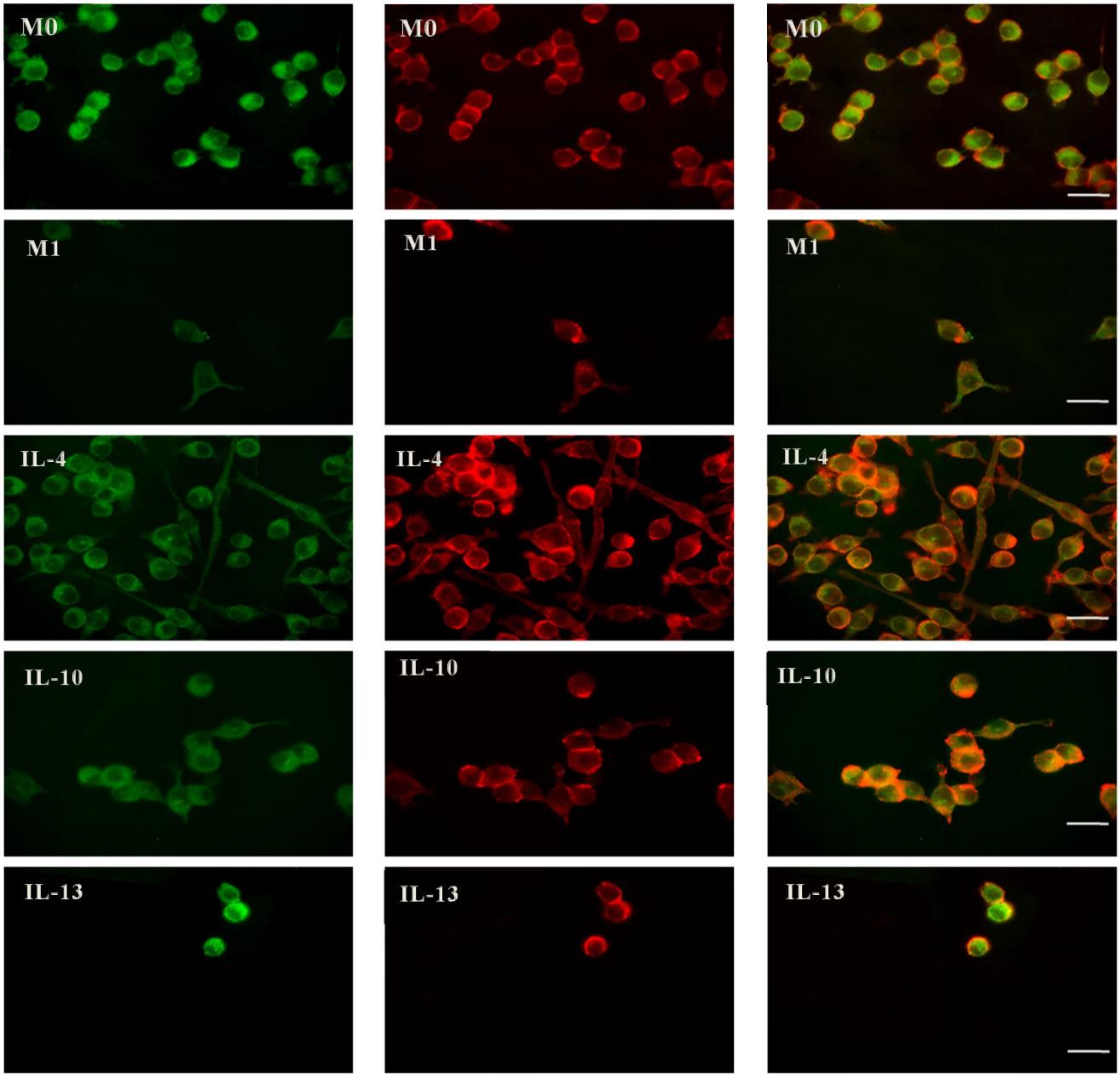

Figure 21: Immunofluorescent images of polarized and un-polarized J774A.1 macrophages cells show morphological changes and cytoskeleton immunostaining at 48 hours prior to- HSV-1 infection.

Green fluorescence (FITC, tubulin) images show unpolarized and polarized macrophages that were fixed and stained with αβ-tubulin antibody for (microtubules arrangement) in the first Colum, red fluorescence (TRITC, F-actin) images show phalloidin (for filamentous actin arrangement) in the second Colum, and the last Colum show the overlay between tubulin and phalloidin staining (Images captured at 60X oil magnification, scale bar =50μm) (n= 9).

M0 control unpolarized

M1 macrophages polarized by LPS and IFN- γ

M2 macrophages polarized by IL-4, IL-10, and IL-13 cytokines

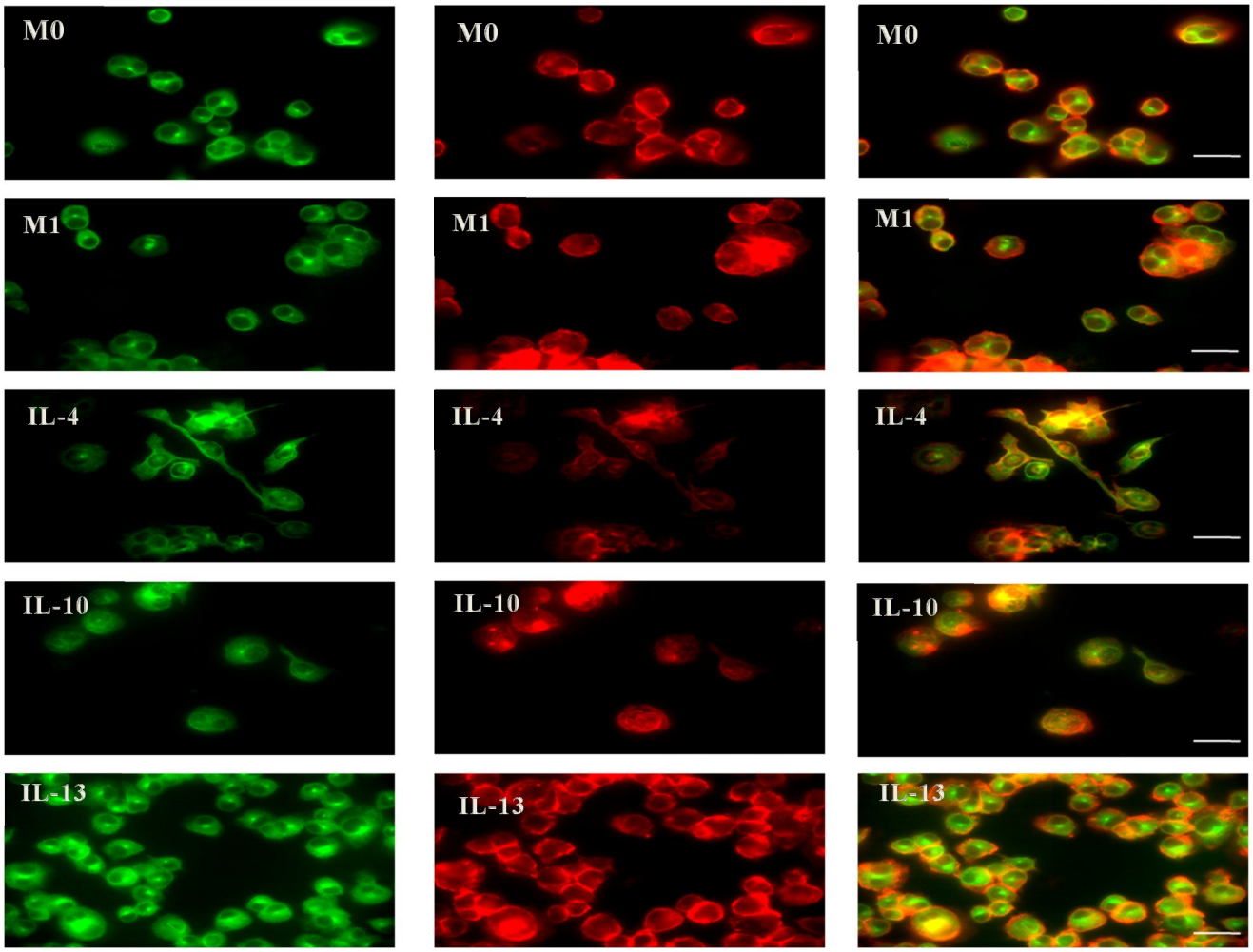

Figure 22: Immunofluorescent images of polarized and un-polarized J774A.1 macrophages cells show morphological changes and cytoskeleton immunostaining at 48 hours after- HSV-1 infection.

Green fluorescence (FITC, tubulin) images show unpolarized and polarized macrophages that were fixed and stained with αβ-tubulin antibody for (microtubules arrangement) in the first Colum, red fluorescence (TRITC, F-actin) images show phalloidin (for filamentous actin arrangement) in the second Colum, and the last Colum show the overlay between tubulin and phalloidin staining (Images captured at 60X oil magnification, scale bar =50μm) (n= 9).

M0 control unpolarized

M1 macrophages polarized by LPS and IFN-γ

M2 macrophages polarized by IL-4, IL-10, and IL-13 cytokines

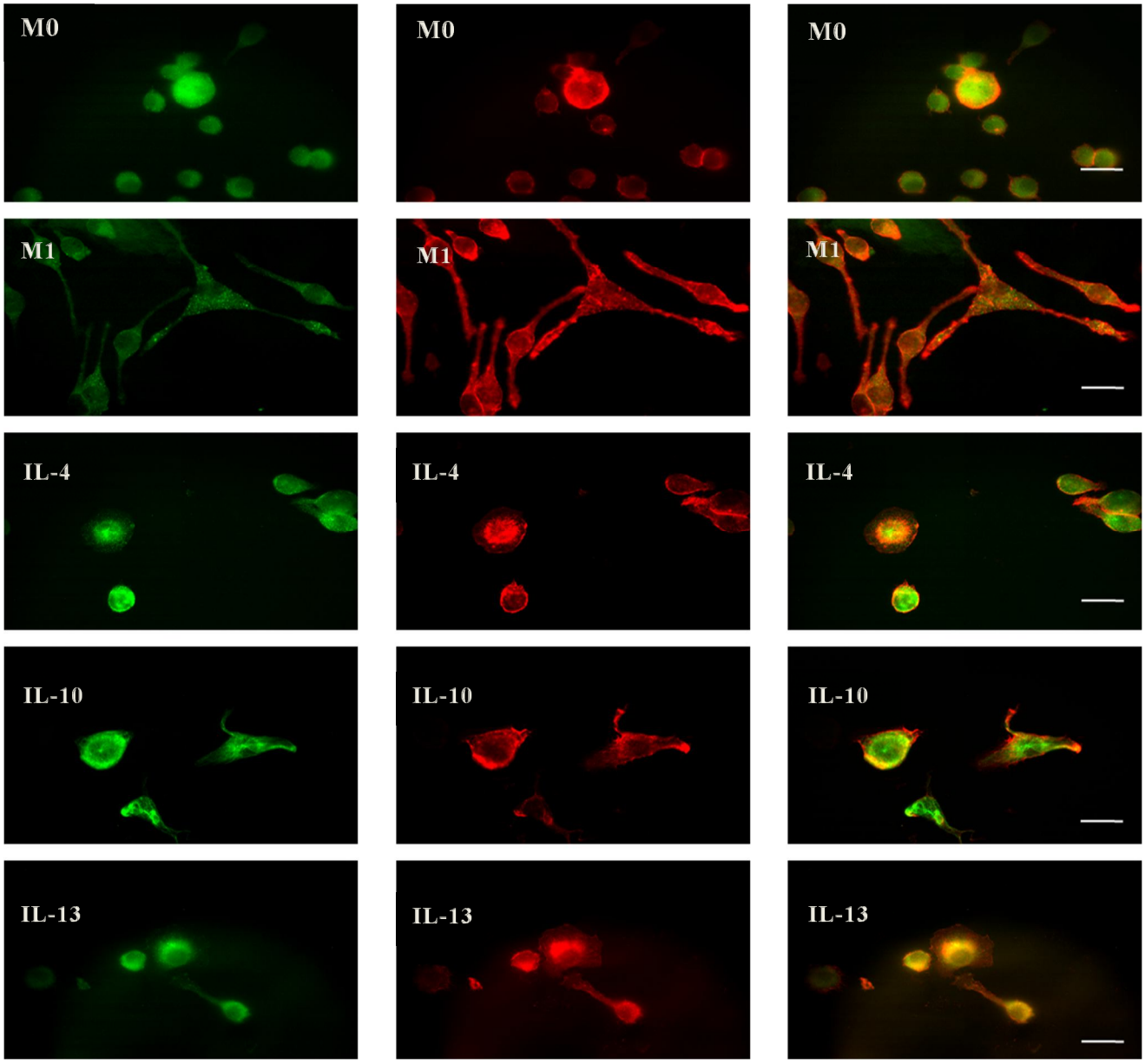

Figure 23: Immunofluorescent images of polarized and un-polarized J774A.1 macrophages cells show morphological changes and cytoskeleton immunostaining at 72 hours prior to- HSV-1 infection.

Green fluorescence (FITC, tubulin) images show unpolarized and polarized macrophages that were fixed and stained with αβ-tubulin antibody for (microtubules arrangement) in the first Colum, red fluorescence (TRITC, F-actin) images show phalloidin (for filamentous actin arrangement) in the second Colum, and the last Colum show the overlay between tubulin and phalloidin staining (Images captured at 60X oil magnification, scale bar =50μm) (n= 9)

M0 control unpolarized

M1 macrophages polarized by LPS and IFN-γ

M2 macrophages polarized by IL-4, IL-10, and IL-13 cytokines

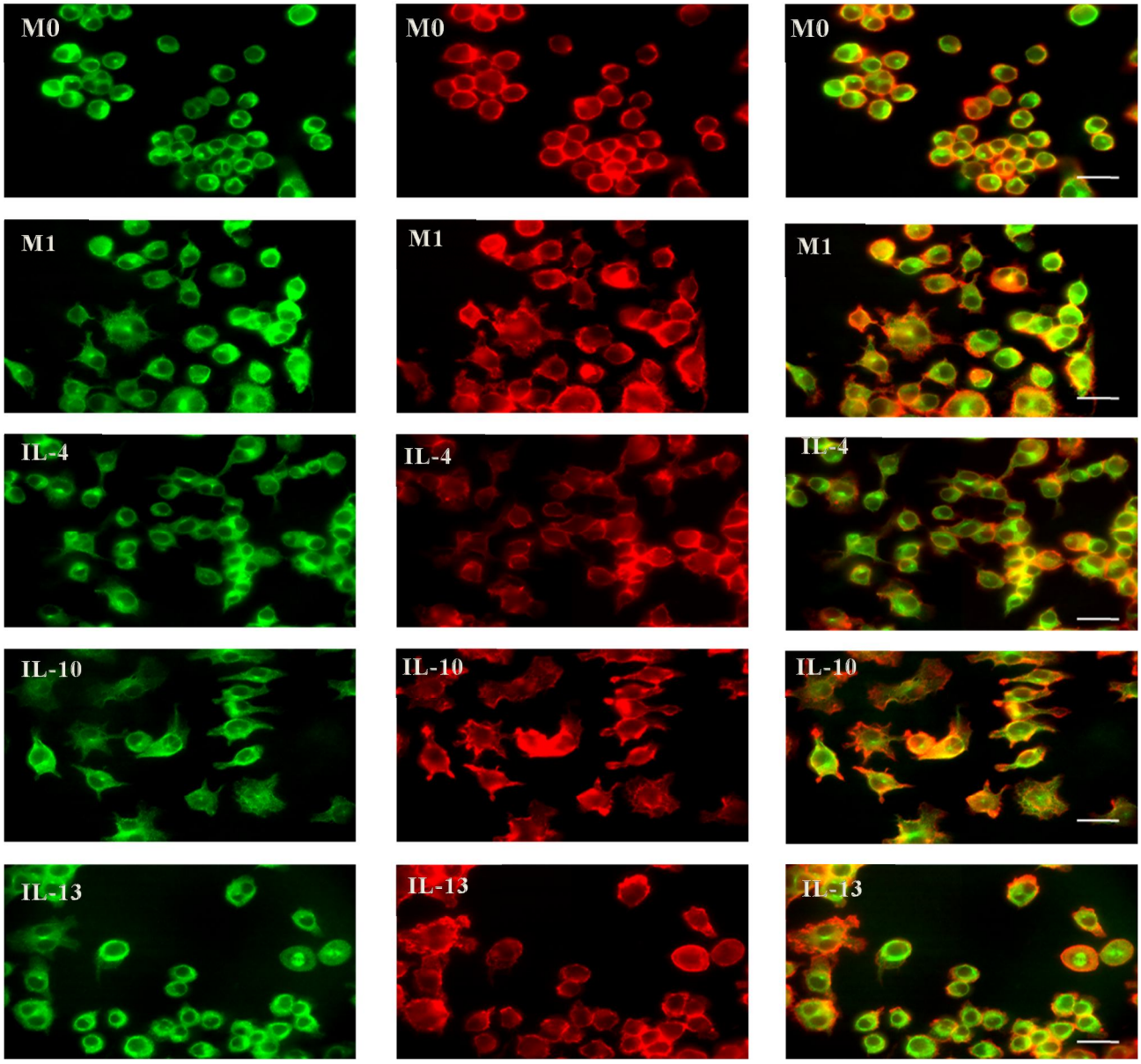

Figure 24: Immunofluorescent images of polarized and un-polarized J774A.1 macrophages cells show morphological changes and cytoskeleton immunostaining at 72 hours after- HSV-1 infection.

Green fluorescence (FITC, tubulin) images show unpolarized and polarized macrophages that were fixed and stained with αβ-tubulin antibody for (microtubules arrangement) in the first Colum, red fluorescence (TRITC, F-actin) images show phalloidin (for filamentous actin arrangement) in the second Colum, and the last Colum show the overlay between tubulin and phalloidin staining (Images captured at 60X oil magnification, scale bar =50μm) (n= 9)

M0 control unpolarized

M1 macrophages polarized by LPS and IFN-γ

M2 macrophages polarized by IL-4, IL-10, and IL-13 cytokines